

掲載予定雑誌名: Brain Structure and Function (平成 29 年掲載予定)

Title:

Shaping somatosensory responses in awake rats:
cortical modulation of thalamic neurons

Daichi Hirai¹, Kouichi C. Nakamura¹, Ken-ichi Shibata¹, Takuma Tanaka², Hiroyuki
Hioki¹, Takeshi Kaneko¹, and Takahiro Furuta^{1*}

*1. Department of Morphological Brain Science, Graduate School of Medicine, Kyoto
University, Kyoto 606-8501, Japan.*

*2. Department of Computational Intelligence and Systems Science, Interdisciplinary
Graduate School of Science and Engineering, Tokyo Institute of Technology, Yokohama
226-8502, Japan*

Keywords: Barrel cortex, Corticothalamic, Thalamus, Burst and tonic modes, Lesion

***Corresponding Author:**

Dr Takahiro Furuta
Department of Morphological Brain Science, Graduate School of Medicine
Kyoto University
Kyoto 606-8501
Office: +81-75-753-4331
Fax: +81-75-753-4340
Email: furuta@mbs.med.kyoto-u.ac.jp

Abstract

Massive corticothalamic afferents originating from layer 6a of primary sensory cortical areas modulate sensory responsiveness of thalamocortical neurons and are pivotal for shifting neuronal firing between burst and tonic modes. The influence of the corticothalamic pathways on the firing mode and sensory gain of thalamic neurons has only been extensively examined in anesthetized animals, but has yet to be established in the awake state. We made lesions of the rat barrel cortex and on the following day recorded responses of single thalamocortical and thalamic reticular neurons to a single vibrissal deflection in the somatosensory system during wakefulness. Our results showed that the cortical lesions shifted the response of thalamic neurons towards bursting, elevated the response probability and the gain of thalamocortical neurons, predominantly of recurring responses. In addition, after the lesions, the spontaneous activities of the vibrissa-responsive thalamic neurons, but not those of vibrissa-unresponsive cells, were typified by waxing-and-waning spindle-like rhythmic spiking with frequent bursting. In awake rats with intact cortex, identified layer 6a corticothalamic neurons responded to a single vibrissal deflection with short latencies that matched those of layer 4 neurons, strongly suggesting the existence of an immediate corticothalamic feedback. The present results show the importance of corticothalamic neurons in shaping thalamic activities during wakefulness.

Introduction

The massive corticothalamic feedback projection from layer 6a is a hallmark structure of the mammalian thalamocortical circuit (Deschênes et al. 1998; Briggs and Usrey 2008; Thomson 2010). The topographic and reciprocal connection between the cortex and thalamus (Sherman and Guillery 1996; Deschênes et al. 1998; Alitto and Usrey 2003) places layer 6a corticothalamic neurons strategically for dynamically modulating the information flow of ascending sensory signals through the thalamus in accord with ongoing behavioral demands. It has been shown that the corticothalamic inputs shape receptive fields (Murphy and Sillito 1987; Yan and Suga 1996; Zhang et al. 1997; Temereanca and Simons 2004; Li and Ebner 2007; Jones et al. 2012) and modulate gain, probability and temporal patterns of sensory responses of thalamocortical neurons (Przybylski et al. 2000; Rivadulla et al. 2002; Temereanca and Simons 2004; Andolina et al. 2007; Briggs and Usrey 2008, 2011). In comparison with the ascending “driver” afferents, which carry sensory information, corticothalamic afferents from layer 6a are classified as “modulators” (Sherman and Guillery 1998, 2006). The net effect of layer 6a corticothalamic modulators on thalamocortical neurons is a complex amalgam of monosynaptic glutamatergic excitation and disynaptic feedforward inhibition via GABAergic neurons in the thalamic reticular nucleus (TRN) (Mease et al. 2014; Crandall et al. 2015), challenging our understanding of their roles.

Thalamocortical neurons operate in tonic or burst firing modes which demonstrate that a thalamocortical neuron can respond to the same input stimuli with critically different outcomes (Sherman 2001a; Swadlow and Gusev 2001). Whereas the tonic mode operates as a faithful relay of sensory input (Ramcharan et al. 2000), the burst mode functions as a non-linear transformation of input by responding with

characteristic bursts of action potentials, *i.e.* low-threshold Ca^{2+} spike (LTS) bursts (Jahnsen and Llinás 1984a, b; Sherman 2001a; Weyand et al. 2001). Layer 6 corticothalamic input contributes to the control the resting membrane potentials of thalamic neurons, and can thereby switch their firing mode via voltage-gated T-type Ca^{2+} channels, which has been shown in slice preparation (McCormick and von Krosigk 1992). Activation of layer 6 corticothalamic input *in vivo* under anesthesia is sufficient to shift burst firing of thalamocortical neurons to tonic firing by depolarizing the resting membrane potentials (Wang et al. 2006; Mease et al. 2014). However, given that net effect of corticothalamic inputs is activity-dependent and can be excitatory or inhibitory (Mease et al. 2014; Crandall et al. 2015) and that brainstem-derived modulatory inputs can also change the resting membrane potentials (Sherman 2001a), it remains to be established whether corticothalamic modulators are necessary for maintaining thalamocortical neurons in tonic firing mode during wakefulness.

The present knowledge about the function of corticothalamic neurons in shaping sensory responses of thalamocortical neurons largely relies on experiments in anesthetized animals. Whereas accumulating evidence underscores their modulatory roles on the one hand (Briggs and Usrey 2008), lesion, inactivation or activation of corticothalamic inputs has often resulted in little, subtle, or no changes in the response properties of thalamocortical neurons (Kalil and Chase 1970; Diamond et al. 1992; Ghosh et al. 1994; Reichova and Sherman 2004; Olsen et al. 2012; Lien and Scanziani 2013; Li et al. 2013; King et al. 2016). Thus, the magnitude of corticothalamic modulation of thalamic responses varies across studies, and the lack of consensus has been obscuring their functions. However, corticothalamic influences may be understood better by recording neuronal activities in awake animals, not only because thalamic

neurons are locked in the burst mode under deep anesthesia (Sherman 2001a; Mease et al. 2014), but also because corticothalamic neurons become unresponsive or even silent by anesthesia (Kwegyir-Afful and Simons 2009; Briggs and Usrey 2011). In addition, corticothalamic modulation of thalamic response probabilities may be associated with a shift in firing mode under anesthesia (Mease et al. 2014). Thus, it is imperative to elucidate the role of the corticothalamic pathways in controlling sensory response profiles of thalamocortical neurons in awake animals.

In the present study, the day after making the lesion of the barrel field of somatosensory cortex (S1), we addressed how this impacts on the firing mode and sensory response profiles of thalamocortical and thalamic reticular neurons in the rat somatosensory system during wakefulness.

Materials and Methods

Animal preparation. The Ethical Committee for the Institute of Laboratory Animals, Graduate School of Medicine, Kyoto University, approved all experimental protocols. All efforts were made to minimize the number of animals used and the animal suffering. Adult Sprague-Dawley rats (250–350 g, male) were handled briefly and adapted to a plastic cylinder in their home cage. The cylinder mimics the shape of a metal cylinder that is used to contain the animal's body while the head is fixed to a stereotaxic apparatus for recording. A light-weight, sliding head attachment (Narishige) and steel screw electrodes for electrocorticography (ECoG) were surgically attached to the skull with screws and dental resin cement (Miky plus; Nissin) under anesthesia produced by an intraperitoneal injection of chloral hydrate (35 mg/100 g body weight) and buprenorphine HCl (0.1 mg/kg) for postoperative analgesia. After surgical recovery, the rats were deprived of drinking water in their home cages, where food was available *ad libitum*. The rats were gradually trained for 3 to 5 days to become accustomed to head fixation in the stereotaxic apparatus. During the training period, water had been available only at the training apparatus. Once animals became habituated, the rats were subjected to the second surgery under chloral hydrate anesthesia, and a small (1–1.5 mm) hole was made in the skull above the recording area. The hole was covered with dental resin cement and/or silicone sealant (DentSilicone-V; Shofu) until the recording experiment.

S1 lesion. The day before recording from the ventral posteromedial nucleus (VPM) or TRN, *i.e.* on the same day as the second surgery mentioned above, cortical area S1 was lesioned by the deposition of a small crystal of silver nitrate over the pia. The crystal

was left in place for 15 min to allow diffusion of the chemical to the deep layers. Then, the cortical surface was rinsed with an excess of saline. The rat was given buprenorphine HCl (0.1 mg/kg) for postoperative analgesia. Silver nitrate is a strong cauterizing agent that burns tissue, and this lesion method was previously shown to produce an immediate, irreversible suppression of cortical activity (Lavallée et al. 2005; Urbain and Deschênes 2007). Since recordings were carried out the day after silver nitrate application, this method of cortical lesion does not involve long-term (>1 day) adaptation of circuitry to the lesion. After the end of experiments, sections were processed for Nissl staining, and the extent of lesion was identified (Supplementary Fig. 1).

Vibrissal stimulation. The left facial nerve was blocked at the proximal part of buccal and marginal mandibular branches with a combination of local anesthetics (absorbent cotton with 2 % xylocaine gel and 0.2 % tetracaine) to prevent vibrissal movement. Vibrissae were cut 5 mm from the skin. A hand-held probe was used under a dissecting microscope to identify each neuron's principal vibrissa, that is, the one which most effectively evoked a neuronal response. The tip of the vibrissa was then, without glue, loosely held in a thin groove carved at the tip of a wooden toothpick that is attached to a ceramic bimorph bender (Physik Instrumente, Karlsruhe, Germany). The vibrissa was pushed in a given direction at stimulus onset by the bender and returned passively. The vibrissa was pushed in a given direction at the stimulus onset, but returned passively at a neutral position at the stimulus offset. Ramp-and-hold waveforms (rise/fall times, 10 ms; total duration, 500 ms or 200 ms; inter-stimulus interval, 1 s) (Furuta et al. 2011) were used to deflect the vibrissa from its resting positions in four directions spanning

360° (*i.e.*, in 90° increments relative to the vibrissal rows). Stimuli were repeated 20 times, the probe was rotated by 90°, and the sequence was repeated to evoke action potentials in the thalamus and S1.

Recording of cells in the thalamus. The day after the second surgery, single units were recorded extracellularly with a micropipette (tip diameter ~1.2 µm) filled with a solution of potassium acetate (0.5 M) and either 2 % tetramethylrhodamine (TMR)-cadaverine (A1318; Life Technologies) or 2 % TMR-biocytin (T12921; Life Technologies) with 0.0003 % Triton-X without anesthesia, under ketamine/xylazine anesthesia (75 mg/kg, 5 mg/kg, respectively) for comparison with those reported previously under anesthesia. For recording in the VPM, TRN and principal nucleus of the trigeminal complex (PrV), the pipette was inserted vertically through the hole in the skull into the recording area (VPM: 3–4 mm posterior, 2–4 mm lateral to bregma; Rt: 2–3 mm posterior, 3–4 mm lateral to bregma; PrV: 9–10 mm posterior, 2.5–3 mm lateral to bregma) with a microdrive that was installed on a stereotaxic frame (SR-8N; Narishige). The juxtacellularly-recorded signal was amplified with an intracellular amplifier (IR-183; Cygnus Technology) and sampled at 10 kHz (bandpass filter, 0.1–3 kHz). To monitor cortical state, ECoG recordings were simultaneously made from the dural surface of S1 of the right hemisphere through stainless steel screw electrodes with the cerebellum as a reference (Supplementary Fig. 2). We advanced the tip of the recording electrode in 2 µm steps while monitoring the occurrence of spontaneous action potentials. Once we found a neuron, the principal vibrissa was determined as described above. Action potentials were recorded initially as negative-orientated waveforms but upon additional advance of the electrode (generally 3–5 steps) units were recorded as positive-orientated

waveforms of 1–3 mV. When the principal vibrissa of a neuron was determined with a hand-held probe as above, a piezoelectric stimulator was subsequently used to achieve detection of subtle, but significant, neuronal activities of that neuron in response to deflections of the principal vibrissae. We recorded stimulus-evoked activities of VPM and TRN neurons that were responsive to vibrissal stimuli with the piezo stimulator. We also recorded spontaneous activities of VPM and TRN neurons that were responsive (Fig. 5-7) and unresponsive (Fig. 7) to deflections of the principal vibrissae. VPM neurons were included in the analysis only when they responded strongly to one vibrissa, in order to avoid neurons in the posterior medial nucleus (POm).

Recording of cells in S1. Cortical recordings were made in the same way as thalamic recordings except the following. For recording in the right barrel cortex (stereotaxic coordinates: 3.3 mm posterior to bregma and 4.5–5.0 mm lateral from the midline), the micropipette was lowered at an angle of 25–40° from the vertical to record cortical cells (depth: 0–1900 µm below the pia) in barrel columns of the B–E rows after identifying single vibrissal selectivity of the presumed layer 4 neurons (depth: 650–950 µm) in the recording track. The receptive field of each neuron was mapped by stimulating vibrissae with a hand-held probe, and the principal vibrissa was determined for each neuron in barrel columns as the vibrissa that evokes responses with the largest amplitude. When we found neurons in layer 4 responsive to multiple vibrissae, we abandoned the recording track and moved on to next penetration. By keeping the angle of penetration constant while exploring the same cortical region, depth readings from the microdrive proved to be a reliable indicator of unit locations (Supplementary Fig. 3). Because the aim of these experiments was to identify the response properties of cortical neurons in

each layer, we primarily sought to record all well-isolated units, when a unit was encountered. For comparison, we further examined the responsiveness of neurons in the barrel cortex to vibrissal stimulation under ketamine (75 mg/kg; xylazine, 5 mg/kg) anesthesia.

Labeling of thalamic and cortical cells. We recorded spiking activity of single neurons one by one along one penetration track. After recording the last neuron of each track, we induced anesthesia (v/v, stage II–III) quickly with 1–2 % isoflurane through a custom-made facemask over the animal’s snout and juxtacellularly labeled the last neuron with the neuronal tracer by applying positive current pulses (1–6 nA, 50% duty cycle at 1 Hz, for 20–30 min) (Pinault 1996) for identification of unit locations and visualization of the neuronal structure. Thus, while most of the juxtacellularly-recorded neurons were not identified anatomically, the locations of unidentified neurons were readily extrapolated from the labeled neurons at the end of the track and the depth reading of the microdrive for each neuron. Neuronal structures were determined only for layer 6a neurons. To ensure the stability for cell labeling, we induced anesthesia with 1–2 % isoflurane after recording the last neuron of each track. The rats were allowed to recover from anesthesia for at least 2 h prior to the subsequent recording experiment. The penetrations were separated from each other by >600 μm for better identification of recording sites. After completing this protocol, the skull hole was covered, all rats were given subcutaneous ketoprofen (Anafen; Merial Inc), and they were returned to the animal facility.

Histology and cell reconstruction. Two to three days later or 2–3 h later for TMR-cadaverine or TMR-biocytin labeling, respectively, rats were perfused under deep anesthesia with PBS, followed by 200 mL of 3 % paraformaldehyde, 75 % saturated picric acid, 0.02 % glutaraldehyde in phosphate buffer (0.1 M), and 0.1 M Na₂HPO₄ (adjusted with NaOH to pH 7.0). After perfusion, brains were post-fixed for 2 h in the same fixative at room temperature, cryoprotected in 30 % sucrose at 4 °C, and cut at 40- μ m thickness into free-floating coronal sections on a freezing microtome for verification of recording sites or lesions.

For TMR-labeled neurons, the free-floating sections were coverslipped with PBS without drying, and native fluorescence of TMR in wet tissue was observed under epifluorescence microscopy (Axiophot; Carl Zeiss). The brain sections that contained one or more TMR-labeled neurons were processed for further immunoperoxidase staining. All the following incubations were carried out at room temperature. All the serial sections were incubated overnight with 0.5 μ g/mL affinity-purified rabbit antibody to TMR (Kaneko et al. 1996) and with 1.0 μ g/mL affinity-purified guinea pig antibody to vesicular glutamate transporter 2 (VGluT2) (Fujiyama et al. 2001) in 5 mM sodium phosphate (pH 7.4)-buffered 0.9 % saline (PBS) containing Triton X-100 (PBS-X). After a wash in PBS-X, the sections were incubated for 1 h with goat antibody to rabbit IgG (1/200; 0112-0881; Capel), and then for 1 h with rabbit PAP (1/400; 323-005-024; Jackson ImmunoResearch). After a rinse in 0.1 M phosphate (pH 7.4)-buffered 0.9 % saline (PB), we applied the biotinylated tyramine-glucose oxidase (BT-GO) method for signal amplification (Kuramoto et al. 2009). The sections were incubated for 30 min in the BT-GO reaction mixture containing 0.5 M BT, 3 mg/mL of GO (257 U/mg; 16831-14; Nacalai Tesque), 2 mg/mL of beta-D-glucose, and 1 %

bovine serum albumin in 0.1 M PB (pH 7.4), followed by a wash with PBS. Subsequently, the sections were incubated for 1 h with ABC Elite (1:100; Vector Laboratories) in PBS-X, and the bound peroxidase in ABC Elite was then developed to brown by reacting for 30–60 min with 0.02 % diaminobenzidine-4HCl (DAB; 347-00904; Dojindo) and 0.0001 % H₂O₂ in 50 mM Tris-HCl (pH 7.6) to reveal TMR immunoreactivity. Subsequently, all the sections were incubated for 2 h with 10 µg/mL biotinylated goat antibody to guinea pig IgG (BA-7000; Vector) in PBS-X containing 1 % normal rabbit serum and then for 1 h with 1/100-diluted ABC-Elite in PBS-X. Finally, peroxidase in ABC-Elite was developed red/fuchsia by a 15 min incubation with 0.01 % Tris-aminophenylmethane (TAPM; 35423-74; Nacalai Tesque) (Kaneko et al. 1994), 0.07 % p-cresol (09708-22; Nacalai Tesque), and 0.002 % H₂O₂ in 50 mM Tris-HCl (pH 7.6) to visualize VGluT2 immunoreactivity. All the stained sections were serially mounted onto the gelatinized glass slides and dried. After washing in running water for 10 min to remove the PBS and drying overnight, the sections were cleared in xylene and then coverslipped. Labeled neurons were drawn with a camera lucida apparatus; drawings were scanned, redrawn in Illustrator CS2 (Adobe Systems), and superimposed on the image of the array of barrels visualized by immunostaining for VGluT2 (TAPM/p-cresol) after appropriate rescaling. Photomicrographs were taken with a Spot RT camera (Diagnostic Instruments) and imported into Photoshop 7.0 (Adobe Systems) for contrast and brightness adjustments.

After reconstruction of TMR-labeled neurons, or in verifying the extent of S1 lesions across serial sections, the relevant sections mounted on gelatinized glass slides were counterstained for Nissl with 0.2% cresyl violet for visualization of the

cytoarchitecture. Cortical layers and barrels were determined according to the Nissl staining and VGluT2 immunoreactivity (Supplementary Fig. 3).

Data analysis. Spike events elicited by vibrissal deflections were collected as peri-stimulus time histograms (PSTHs) of 20 trials with a bin width of 2 ms. The response magnitude was defined as the maximum spike number in 200 ms after stimulus onset among the tested 4 tested directions. We identified the preferred direction of each cell and used this data in the following analyses. For a given stimulus, spike times were aligned to the stimulus onset time and the periods of 0–20 ms and 50–200 ms after stimulus onset were considered as ‘onset period’ and ‘late period’ respectively. The probability of response to vibrissal stimulation was determined as the percentage of trials with a successful spike response (regardless of the number of spikes per response) to all the trials. We defined response onset of each neuron as either the first 1 ms bin (post-stimulus) displaying counts that significantly exceeded the level of the spontaneous activity by the mean + 3 SD of the level calculated over a pre-stimulus time window of 200 ms or as the first two consecutive bins displaying significantly larger counts (mean + 2 SD) than the spontaneous activity level. When a response PSTH of a neuron exhibited either a single bin exceeding the mean + 3 SD of the spontaneous activity or two consecutive bins exceeding the mean + 2 SD in onset period or late period, we considered that the neuron responded in the period. Recorded neurons were classified into three response types (onset type, recurrent type, late type) according to the presence of sensory responses in onset period and late period: onset type, recurrent type and late type neurons respectively exhibited responses only in onset period, in both onset and late periods, and only in late period. Previous quantitative

analyses have shown that LTS bursts are preceded by a silent period (50–100 ms) (Lu et al. 1992). Accordingly, LTS bursts were identified on the basis of previously defined criteria for LTS bursts of rat thalamocortical neurons in extracellular unit recordings: at least 2 action potentials with an inter-spike interval (ISI) of ≤ 4 ms for the VPM (Lacey et al. 2007; Nakamura et al. 2014) or ≤ 10 ms for the TRN but with a preceding silent period of > 50 ms (Lu et al. 1992; Ramcharan et al. 2000). The offset timing of the burst was also defined as in previous studies: ISI of > 10 ms for the VPM (Fanselow et al. 2001) and ISI for > 20 ms for the TRN (Marlinski and Beloozerova 2014). The percentage of successful trials with LTS bursts was calculated as the number of successful trials that include an LTS burst divided by the total number of trials with a successful spike response. As to cortical recording, we found only 6 neurons with late responses, so we focused our analyses to onset responses. When a response PSTH of a neuron exhibited either a single bin exceeding the mean + 3 SD of the spontaneous activity or two consecutive bins exceeding the mean + 2 SD in onset period, we considered that the neuron was responsive. In analyzing the oscillatory nature of spontaneous spiking activity, we used a multitaper FFT (Mitra and Pesaran 1999) with a fixed frequency resolution of 0.4 Hz to obtain the power spectral density (PSD) of spike trains. The PSD was normalized by the total power of all bins (0.3–100 Hz; bin, 0.1 Hz). Data were analyzed with MATLAB (MathWorks), IGOR Pro (WaveMetrics), and Excel (Microsoft) software. Results are reported as mean \pm SD.

Statistical analysis. Non-parametric tests were adopted throughout, because some of our data did not satisfy requirements for parametric tests. The Mann-Whitney *U*-test was used for unpaired samples, whereas the Wilcoxon signed-rank test was used for paired

samples. Fisher's exact test was used to determine whether there is a difference in proportions between two populations in 2×2 contingency table with small sample sizes. For corrections for multiple comparisons, we used the Bonferroni–Holm correction (Holm 1979), which controls the family-wise error rate at level. Significance level was set at $p < 0.05$.

Results

Sensory responses of VPM neurons in rats with or without cortical lesions

To establish the effect of cortical feedback onto thalamic relay functions during waking, we compared the responses evoked by vibrissal stimuli in VPM neurons in rats having lesions in the barrel cortex with the responses in control animals (Fig. 1). In order to rule out the possibility of residual corticothalamic function, we made large cortical lesions that cover the whole barrel cortex with silver nitrate, which allows us to control the size of lesions (Lavallée et al. 2005) (Supplementary Fig. 1). In the control rats (19 rats), we recorded 71 single units that responded to the deflection of their principal vibrissae in the VPM. Of these 71, 62 neurons showed short response latencies (5–18 ms) to the vibrissal deflection (Supplementary Fig. 4). These immediate spikes at short latencies (0–20 ms) were defined as “onset responses”. They are considered as neuronal activities driven by ascending input from the PrV (Supplementary Fig. 5, 6 rats). We also observed “late responses” that occurred between 50 ms and 200 ms after the stimulus onset in 23 of the 71 neurons (Supplementary Fig. 4). Additionally, the responses often included LTS bursts in both the onset and late periods (small red bars in Fig. 1E). The recorded neurons were classified into three groups according to the presence of the onset and late responses: “onset type” neurons that exhibited only onset responses (48 of 71 recorded cells), “recurrent type” neurons that had both onset and late responses (14 of 71), and “late type” neurons that showed only late responses (9 of 71). Because neurons in the PrV ($n = 29$) exhibited responses of short latencies (7.38 ± 2.98 ms) but not any discharges in the late period (Supplementary Fig. 5), the late activities in VPM neurons are considered to be caused by intra-thalamic and/or corticothalamic circuitry.

In the VPM of 7 rats with a barrel cortex lesion, we recorded 27 single units responding to the deflection of their principal vibrissa with the same vibrissal stimuli (Fig. 1G–K). Figures 1G and 1H show the extent of a cortical lesion caused by silver nitrate application on the surface of the S1. As indicated by the loss of Nissl staining in coronal sections of the rat brain, lesions extended across the barrel field in the right S1 (Supplementary Fig. 1). VPM neurons in the lesioned rats also responded to vibrissal deflections in both the onset and late periods (7 rats). Of 27 VPM neurons, 10 and 17 were classified as onset type and recurrent type neurons, respectively, while no late type neurons were found in the lesioned rats (Fig. 1I–L). The cortical lesions resulted in a higher probability of a response to the sensory stimulus in the VPM both in the onset and late periods ($p = 3.5 \cdot 10^{-5}$, $p = 1.0 \cdot 10^{-5}$, respectively, Mann-Whitney *U*-test, Fig. 2A), and led to more spikes being included within the LTS bursts during the onset period ($p = 2.9 \cdot 10^{-5}$, Mann-Whitney *U*-test, Fig. 2B). Moreover, a larger proportion of VPM neurons were responsive during the late period in lesioned rats than in control rats ($p = 0.01$, Fisher's exact test, Fig. 1L). The augmentation of VPM responses was confirmed in both the onset and late periods at a population level (Fig. 2C). The firing rates of VPM neurons in the onset and late periods were significantly higher in the lesioned rats than in the control rats (Fig. 2D). Even when we considered only the spikes that were included in LTS bursts for the population PSTH, vibrissal stimulus-evoked responses were significantly increased in the lesioned rats (Fig. 2E, F). Thus, the response profiles of VPM neurons of awake rats with a cortical lesion showed a predominance of recurrent type neurons, augmentation of responses in both the onset and late periods, and increased occurrence of LTS bursts in the onset period.

Responses of TRN neurons in rats with or without cortical lesions

The cortical lesion caused an increase of VPM responses, suggesting that the net effect of corticothalamic excitatory input may be to suppress VPM neuronal activity in the intact brain. It is well known that, corticothalamic axons to the VPM send collaterals to the TRN (Bourassa et al. 1995), which in turn sends inhibitory axons to VPM neurons (Lee et al. 1994). Hence, corticothalamic input may suppress sensory responses of thalamic relay neurons by activating the TRN. If so, then the cortical lesion can be expected to decrease the responses of TRN neurons. We thus compared sensory-evoked responses of TRN neurons between control rats and lesioned rats (Fig. 3). Neurons in the TRN were identified on the basis of their long-lasting (60 ± 20 ms) burst discharges as previously reported (Marlinski and Beloozerova 2014). Of 29 TRN neurons recorded in control rats, 19 were classified as onset type neurons, and the other neurons were recurrent type neurons (Fig. 3D–F, 3L, 9 rats). In lesioned rats, the majority of the recorded TRN neurons (17 of 26) were recurrent type neurons (Fig. 3I–L). The ratio of recurrent type neuron in the lesioned rats was significantly larger than that in the control rats ($p = 0.01$, Fisher's exact test, Fig. 3L). No late type neuron was found in the TRN. After the cortical lesion, a statistically significant increase in the probability of a sensory response was observed during the late period, but not during the onset period (onset period; $p = 0.95$, late period; $p = 0.03$, Mann-Whitney U -test, Fig. 4A). Figure 4B shows that a larger proportion of TRN spikes were included in LTS bursts in cortex-lesioned rats than in control rats (onset period; $p = 2.0 \cdot 10^{-4}$, late period; $p = 0.04$, Mann-Whitney U -test). Population PSTHs of TRN neuron responses (Fig. 4C) show that TRN responses may be increased, but never decreased, by the cortical lesion throughout the

response time course. Statistical analyses (Fig. 4D) indicated that the cortical lesions significantly increased the response magnitude of TRN neurons in both the onset and late periods ($p = 0.03$, $p = 0.01$, respectively, Mann-Whitney U -test). We also confirmed that the cortical lesions elevated TRN responses as LTS bursts (onset period; $p = 0.03$, late period; $p = 0.03$, Mann-Whitney U -test, Fig. 4F). These results clearly show that the cortical lesion increased TRN responses, contrary to the prediction of the above hypothesis. Thus, this raises the question as to what other circuit mechanisms may underlie the apparent suppression of VPM responses by corticothalamic input in the intact brain. Because facilitatory corticothalamic influence was induced by repetitive activation of the corticothalamic circuit *in vitro* (Crandall et al. 2015), we examined time-dependent change of neural responses during the sequential vibrissal stimulation by comparing response magnitudes in the first half (10 deflections) of the 20 deflections with those in the latter half (10 deflections). No statistically significant difference was observed between the halves (Supplementary Fig. 6). This inconsistency between the previous and present studies might be explained by the difference in the stimulus frequencies: 10 Hz (Crandall et al. 2015), and 1 Hz in the present study.

Cortical lesion led to spontaneous oscillatory firing of VPM and TRN neurons

The present results clearly show that LTS burst firing is augmented in both the VPM and TRN neurons following cortical lesions. Because LTS bursts rely on strong depolarization caused by activation of T-type Ca^{2+} channel, which requires long enough hyperpolarization of the resting membrane potential for its de-inactivation beforehand (Jahnsen and Llinás 1984a, b), the increase of LTS bursts in the lesioned rats may be explained by elimination of corticothalamic afferents, whose excitatory actions could

limit the hyperpolarization of thalamic neurons in intact animals. If corticothalamic inputs modulate thalamic activity by controlling the baseline membrane potential of each thalamic neuron, the cortical lesion should influence the spontaneous thalamic activity as well. Figure 5 shows the results of the analyses for the effect of cortical lesion on spontaneous activities in the VPM and TRN. In intact rats, VPM neurons and TRN neurons exhibited spontaneous discharges of a moderate firing rate (mean spontaneous firing rate of 26 VPM neurons in 7 rats, 6.6 ± 4.9 Hz; that of 24 TRN neurons in 6 rats, 15.1 ± 7.7 Hz) during the awake state as confirmed by the desynchronized ECoGs. Autocorrelograms (Fig. 5B, E) as well as flat power spectra of spike trains (Fig. 5C, F) illustrate that typical VPM (Fig. 5A–C) and TRN (Fig. 5D–F) neurons in control rats did not have an oscillatory component in their activities. In contrast, clear oscillations in the range of 4–15 Hz were observed both for typical VPM and TRN neurons of cortex-lesioned rats (mean spontaneous firing rate of 22 VPM neurons in 7 rats, 6.8 ± 5.1 Hz; that of 15 TRN neurons in 5 rats, 8.2 ± 5.0 Hz) in the raw traces, the autocorrelograms, and the power spectra, with a frequent occurrence of LTS bursts (Fig. 5G–L). In the scatter plots of inter-spike intervals (ISIs) before and after a spike (Fig. 6A–D), the ~10 Hz oscillatory activities and LTS bursts emerge in the cortex lesioned rats as dense clusters at ranges of ~100 ms and 2–5 ms, respectively. At a population level, a statistically significant increase of power in the alpha frequency band (7–12 Hz) was confirmed both in the VPM and TRN ($p = 7.7 \cdot 10^{-8}$, $p = 1.8 \cdot 10^{-6}$, respectively, Mann-Whitney *U*-test, Fig. 6E–H). Statistical tests also confirmed that cortex-lesioned rats showed more LTS burst activities than control rats (VPM; $p = 1.7 \cdot 10^{-7}$, TRN; $p = 1.5 \cdot 10^{-6}$, Mann-Whitney *U*-test, Fig. 6I, J). Thus, cortical lesions had

profound effects on spontaneous firing patterns of VPM and TRN neurons, including prominent oscillatory activities and increased LTS bursts.

Because the deprivation of the barrel cortex induced the strong oscillatory activity in VPM neurons, one may expect that global changes were evoked by the cortical lesion and that oscillatory activities were exhibited across the whole brain. However, the EEG in the cortex-lesioned rats did not show clear alpha-wave and thus do not support presence of the global oscillatory activity (Fig. 7). We further investigated spontaneous firings of thalamic neurons (in the VPM, ventrolateral nucleus (VPL), POm and TRN) which did not respond to the vibrissal stimulation. Figure 7A shows locations of recorded neurons along the pipet penetration track through the POm and VPM in a cortex-lesioned rat. The vibrissa-unresponsive neurons (Cell 1 and Cell 2) in the POm exhibited no oscillatory activity, whereas vibrissa-responsive neurons (Cell 3 and Cell 4) in the same penetration exhibited clear oscillation (Fig. 7A–C). Similar results were obtained even within the TRN (Fig. 7D–F). By examining power spectra of spontaneous activities, it was confirmed that the alpha power of vibrissa-unresponsive thalamic neurons in the cortex-lesioned rats was similar to that of the responsive neurons in cortex-intact rats (VPM: $p = 0.13$, TRN: $p = 0.56$, respectively, Mann-Whitney U -test with Bonferroni–Holm correction, Fig. 7G–J) and significantly lower than that of the responsive neurons in the cortex-lesioned rats (VPM: $p = 1.2 \cdot 10^{-3}$, TRN: $p = 1.3 \cdot 10^{-3}$, respectively, Mann-Whitney U -test with Bonferroni–Holm correction, Fig. 7G–J). These results indicate that the alpha-band oscillatory activity after the lesion of the somatosensory cortex is not a global phenomenon.

Identification of immediate corticothalamic feedback during wakefulness

Finally, to better understand the changes in thalamic activities following cortical lesions, we examined sensory responses of corticothalamic neurons in the intact S1 during wakefulness. Corticothalamic neurons in layer 6a of the sensory cortex are unresponsive or even silent in anesthetized animals, leaving their functions elusive (Kwegyir-Afful and Simons 2009; Briggs and Usrey 2011). Nevertheless, a growing body of evidence, including that from studies of unanesthetized animals, suggests that not only layer 4 neurons but also layers 5/6 neurons are the earliest to respond to sensory stimuli in the primary sensory areas of cortex (Simons 1978; Maunsell and Gibson 1992; de Kock et al. 2007; Constantinople and Bruno 2013; Plomp et al. 2014). Because corticothalamic neurons make up only ~60% of the neurons in layer 6a (Tanaka et al. 2011), it is important to define whether the layer 6a neurons that respond with a short latency to tactile sensory stimuli from the thalamus in the awake rat are corticothalamic cells. To this end, we recorded juxtacellular responses of single neurons across layers in the barrel cortex to single vibrissal deflection using head-fixed awake rats (Fig. 8A, 8B, 49 rats). In awake rats, significant neuronal responses were observed in all layers except for layer 1. Of the 409 single units recorded in the barrel cortex, 127 neurons exhibited phasic responses to the vibrissal stimulation within 40 ms of stimulus onset. The percentages of neurons responsive to vibrissal stimulations were 27.9 %, 58.8 %, 12.3 %, 39.8 %, 21.5 and 0 % in layers 2/3, 4, 5a, 5b, 6a and 6b, respectively. For comparison, we further examined the responsiveness of neurons in the barrel cortex to vibrissal stimulation in anesthetized rats (Fig. 8D, 12 rats) and found that the percentage of neurons in layer 6a responsive to vibrissal stimulation was markedly lower in anesthetized rats than in awake rats (2.9 %, $p = 0.04$, Mann-Whitney U -test with

Bonferroni–Holm correction, Fig. 8E). This demonstrates that isoflurane anesthesia selectively suppresses responsiveness of layer 6a neurons within barrel cortex. Neurons of layer 6a of awake rats exhibited short response latencies ($n = 30$, 13.1 ± 2.5 ms) that matched those in layer 4 ($n = 40$, 14.9 ± 4.2 ms) ($p = 0.18$, Mann-Whitney U -test with Bonferroni–Holm correction, Fig. 8F), *i.e.* the well-established thalamo-recipient layer, among all cortical layers (Fig. 8B, C, F, G, H). This suggests that thalamocortical excitatory input directly drives layer 6a neurons to evoke action potentials. After the unit recordings, the structures of 24 layer 6a neurons were successfully visualized by juxtacellular labeling and *post hoc* histology. Based on their axonal projection targets, we unequivocally identified two groups of layer 6a neurons; corticothalamic neurons ($n = 16$) were identified with their long projection axons reaching the ventral posteromedial thalamic nucleus (VPM) while corticocortical neurons ($n = 8$) projected axons to the ipsilateral cortices or contralateral hemisphere via the corpus callosum, but not to the thalamus (Fig. 8I, K). In addition to the difference of axonal projection, the superimposed images of the dendrites showed that the labeled corticothalamic neurons possessed longer apical dendrites than the corticocortical neurons (Fig. 8M). We found that 7 of 16 (43.8 %) of corticothalamic neurons in layer 6a showed vibrissal stimulus-evoked responses (Fig. 8N). These results based on unequivocally identified corticothalamic neurons shows that the VPM nucleus receives immediate cortical feedback at a short latency during tactile sensation. This tallies with the anatomical finding that layer 6 corticothalamic neurons receive more direct thalamocortical inputs than layer 6 corticocortical neurons in mouse visual cortex (Vélez-Fort et al. 2014). They also reported that layer 6 corticocortical neurons were more active and broadly responsive to drifting sinusoidal gratings than layer 6 corticothalamic neurons, hence

being apparently contradictory to our finding in rat S1. However, the continuous nature of their visual stimuli suggests that layer 6 neurons are constantly activated by both thalamocortical and intracortical inputs, defying direct comparison to our experiments using vibrissal deflection as a discrete event. The absence of cortical responses during the late period (50–200 ms after stimulus onset) might be due to short-term depression of thalamocortical synapses at 10 Hz stimuli, which has been reported in S1 layer 4 (Gil et al. 1997), albeit yet unknown for layer 6. The immediate responsiveness of corticothalamic neurons may serve to adjust thalamic activity dynamically to the ongoing changes in the environment.

Discussion

We have demonstrated that deprivation of corticothalamic feedback by chemical lesions of the S1 results in a clear shift of firing of VPM and TRN neurons towards the burst mode. In addition, single VPM neurons showed increased response probability and gain with a majority of those neurons engaging in recurrent-type responses in response to a single vibrissal deflection (Fig. 9B). Spontaneous activities of VPM and TRN neurons after the loss of cortical input are typified by recurring bouts (7–12 Hz) of LTS bursts separated by pauses of a few seconds (Fig. 9C, D). Finally, we report that identified layer 6a corticothalamic neurons respond to single vibrissal deflection with a short latency in awake rats, whereas corticocortical neurons are not driven by the tactile stimulation, suggesting that the primary sensory cortex sends immediate feedback to the thalamus (Fig. 9A).

Cortical lesions shift firing of VPM and TRN neurons toward burst mode in awake rats

Although it has been shown *in vitro* that corticothalamic excitatory inputs play an important role in depolarizing the resting membrane potentials of thalamocortical neurons and thereby controlling their firing mode (McCormick and von Krosigk 1992), *in vivo* experiments on this issue with drugs, optogenetics and transcranial magnetic stimulation have been varied across studies: some studies reported that activation of cortical inputs affects the firing mode of thalamic neurons (Wang et al. 2006; Mease et al. 2014), while others reported no or little effect of cortical inactivation (Andolina et al. 2007; de Labra et al. 2007) or activation (Olsen et al. 2012). Because corticothalamic inputs can serve direct excitation and/or TRN-mediated feedforward inhibition of

thalamocortical neurons (Crandall et al. 2015), the net effect of corticothalamic input has been elusive. In the present study, we found that, following a cortical lesion, VPM and TRN neurons responded to a vibrissal deflection significantly more often with an LTS burst as the first response during the onset period (<200 ms from stimulus onset) and that they fired more spikes in LTS bursts during spontaneous activity, indicating that the cortical lesion is sufficient to shift firing of VPM and TRN neurons toward burst mode during wakefulness. This shift, together with the opposite shift and underlying depolarization of membrane potentials after optogenetic activation of corticothalamic inputs (Mease et al. 2014), suggests that the net effect of corticothalamic inputs might be depolarizing, since lower resting membrane potentials are associated with increased availability of de-inactivated T-type Ca^{2+} channels, and hence more LTS bursts.

We found that minor subpopulations of VPM and TRN neurons engaged in the burst firing mode during waking even in cortex-intact rats. Although the presence and function of thalamic LTS bursts during wakefulness has been a matter of debate (Sherman 2001b; Steriade 2001), reports of LTS bursts of thalamocortical neurons (Guido et al. 1992; Guido and Weyand 1995; Weyand et al. 2001; Massaux and Edeline 2003; Massaux et al. 2004) are increasing and have also been reported in TRN neurons (Marlinski and Beloozerova 2014) in awake animals. Our finding further corroborates the presence of LTS bursts in the thalamus of awake animals. Thus, as is the case for the opposite shift by corticothalamic activation under anesthesia (Mease et al. 2014), the transition of the firing modes of VPM and TRN neurons in awake rats by cortical lesion was a gradual shift toward bursting in a continuum, rather than a switch between two discrete states, at the population level.

Previous studies on inactivation of the cortex by drugs, optogenetics, or transcranial magnetic stimulation reported little change in the firing mode of thalamocortical neurons under anesthesia (Andolina et al. 2007; de Labra et al. 2007; Denman and Contreras 2015). However, if we can assume that the net effect of cortical input is depolarizing as mentioned above, removal of cortical input may further hyperpolarize the membrane potentials of thalamocortical neurons, which may have been already hyperpolarized by anesthesia, likely leaving them firmly in burst mode without transition. Taken together, our cortical lesions and previous cortical activation studies (Wang et al. 2006; Mease et al. 2014) jointly suggest that corticothalamic inputs can bidirectionally shift the firing mode of thalamocortical neurons.

The impact of corticothalamic afferents on onset response probability of VPM neurons to single vibrissal deflection

Counterintuitive as it may seem, our results show that the deprivation of excitatory cortical input by S1 lesion results in greater response probability (Fig. 2A) and gain (Fig. 2D) of VPM neurons to vibrissal deflection during onset period (0–20 ms after stimulus onset). While the heightened gain is likely attributable to increased burst firing, and hence more spikes, we propose a simple model that takes three different thresholds into account (Fig. 9E, F) to relate the widely accepted theory of firing mode-dependent thalamic gating (Llinás and Steriade 2006; Sherman and Guillery 2013) to the response probability. By definition, this can also explain the absence of late type neurons, *i.e.* those that failed to respond during onset period, in the VPM of cortex-lesioned rats. At rest, during wakefulness, most VPM neurons in cortex-intact rats are in the tonic mode, and hence the vast majority of their T-type Ca^{2+} channels are inactivated due to the

resting membrane potential that is maintained relatively high (~ -60 mV) (Urbain et al. 2015), most likely by baseline activities of corticothalamic inputs (Fig. 8E). EPSPs evoked by lemniscal inputs need to exceed the high threshold (~ -50 mV) of Na^+ channels to elicit a single action potential. Due to fluctuations in the amplitude of lemniscal EPSPs (Sheroziya and Timofeev 2014), the response probability of VPM neurons to a sensory stimulus is maintained around 60 % for the onset response.

After cortical lesion, however, the removal of corticothalamic excitatory tone may lead to a long enough (> 50 ms) hyperpolarization of membrane potentials (Liu et al. 1995; Ramcharan et al. 2000) of VPM neurons below the de-inactivation threshold of T-type Ca^{2+} channels (Jahnsen and Llinás 1984b), making T-type Ca^{2+} channels available for an LTS, *i.e.* a large calcium spike, even during wakefulness (Fig. 9F). The amplitude of a lemniscal EPSP may normally be large enough to reach the low threshold for activation of T-type Ca^{2+} channels (Zhan et al. 1999), thereby faithfully evoking an LTS that exceeds the high threshold of Na^+ channels and is crowned by a burst of action potentials. Indeed, intracellular recordings have demonstrated that de-inactivation of T-type Ca^{2+} channels can make an otherwise subthreshold current injection able to evoke an LTS burst (Lo et al. 1991). The unique properties of T-type Ca^{2+} channels and the baseline corticothalamic glutamatergic tone in a cortex-intact brain during wakefulness may together be necessary to maintain the onset response probability of VPM neurons unsaturated. Activation of corticothalamic neurons under anesthesia not only showed that VPM neurons shift toward tonic firing, but also showed a decline in their response probability (Mease et al. 2014), displaying the opposite effects to our results. Hence, it appears that the unsaturated responsiveness is associated with the tonic mode and may serve to leave room for bidirectional modulation of

response probability of thalamic relays according to the internal state of the cortical circuit. Indeed, optogenetic stimulation of corticothalamic axons at a higher or lower frequency enhances or suppresses thalamic excitability, respectively (Crandall et al. 2015), and the sensory responsiveness of thalamic relay neurons is modulated by specific behavioral contexts (Fanselow et al. 2001; Lee et al. 2008) or attention (O'Connor et al. 2002; McAlonan et al. 2008). Thus, we provide evidence for an important role of corticothalamic input in keeping the response probabilities of VPM neurons unsaturated.

Covert recurrent activities in the thalamus

During wakefulness, VPM and TRN neurons in cortex-lesioned rats showed spontaneous oscillatory firing patterns that are closely reminiscent of spiking activities of thalamic neurons during sleep spindles, even though ECoGs in cortex-lesioned rats showed desynchronized state (Fig. 5, Supplementary Fig. 1). Sleep spindles appear as brief (1–3 s) episodes of waxing-and-waning field potentials within a frequency range of approximately 7–14 Hz recurring every 5–15 s during an early stage of slow wave sleep or under deep anesthesia (Timofeev et al. 2012). VPM and TRN neurons exhibit LTS bursts that are tightly phase-coupled to spindle oscillations (Slézia et al. 2011; Ushimaru et al. 2012). Sleep spindles are considered to originate from the TRN, because they survive in the TRN *in vivo* after the removal of the cortex (Morison and Basset 1945; Villablanca and Schlag 1968; Contreras et al. 1996, 1997) or of all afferents (Steriade et al. 1987), and also because spindle oscillations in the thalamus are abolished when isolated from the TRN (Steriade et al. 1985). Notably, spindle-like oscillations appear in the thalamus in slice preparation without cortical input (von

Krosigk et al. 1993). Although we could not determine whether the rhythmic burst firing of thalamic neurons in cortex-lesioned rats was synchronous, these and our present results imply that the thalamus, particularly the TRN, may possess a covert spindle-like oscillatory mechanism that occurs in the absence of corticothalamic input.

The responses of thalamic neurons to vibrissal deflections in the late period (late responses; 50–200 ms after stimulus onset) is unlikely to be due to the ascending lemniscal input, at least in cortex-intact rats, in which we found no late response at the PrV. Importantly, the proportion of recurrent-type neurons in the VPM and TRN markedly increased following cortical lesion. This suggests that the corticothalamic afferents are suppressing the thalamic late responses that could dilute the impact of onset responses during normal sensory processing (see below; Fig. 9E, F).

The intervals between the onset and late responses of recurrent-type neurons and the intervals of spindle-like spontaneous firing of thalamic neurons are similar (~100 ms) in cortex-lesioned rats. Moreover, both of these activities after cortical lesion are associated with the burst firing mode. Given these similarities, it is tempting to speculate that the responses of recurrent-type neurons might share, in part, the same oscillatory mechanism as the spindle-like spontaneous firing. In sensory response, the synchronized responses of VPM neurons during onset period appear to elicit barrages of LTS bursts of TRN neurons, which may in turn produce large and long lasting (~100 ms) IPSPs in both VPM neurons via recurrent feedback and TRN neurons via lateral inhibition between each other, as they do during spindle-like oscillations in the lateral geniculate nucleus *in vitro* (von Krosigk et al. 1993; Bal et al. 1995a, b; Kim et al. 1997). At the end of such IPSPs, which may be sufficient for de-inactivation of T-type Ca^{2+} channels, thalamocortical neurons may fire post-inhibitory rebound bursts without

excitatory drive (von Krosigk et al. 1993). The loss of corticothalamic glutamatergic tone and resultant shift toward burst mode might facilitate post-inhibitory rebound as late responses. Thus, the present data suggest that, after cortical lesion, presumably hyperpolarized membrane potentials of TRN and VPM neurons may unleash the spindle-like spontaneous firing patterns and late responses thereof, even during wakefulness.

Methodological considerations

We found that responses of S1 layer 6 neurons to the vibrissal stimulation were markedly suppressed in ketamine/xylazine-anesthetized rats in comparison with awake rats. This is in good agreement with previous studies that showed that ketamine or isoflurane anesthesia suppressed layer 6 responses to sensory inputs (Einevoll et al. 2007; Sakata and Harris 2009; Roy et al. 2011; Constantinople and Bruno 2013). On the other hand, responses of layer 6 neurons remained active under urethane anesthesia (Welker et al. 1993; de Kock et al. 2007), indicating that the suppressive effect is dependent on the choice of anesthetics. Overall, these results strongly argue the importance of investigating neural activities in awake states.

We made cortical lesions by applying silver nitrate onto the cortical surface, which led to elimination of not only neurons of all the layers but also fibers from local cortical connections or cortico-cortical connections. Thus, we should take the other effects of the lesions than those described in Figure 9 into account. Besides layer 6 neurons, layer 5 neurons also send their descending axons reaching subcortical structures. Because the PrV receives axonal projections from layer 5 neurons in S1 and is modulated by

electrical stimulations in the S1 (Furuta et al. 2010; Malmierca et al. 2014), the present cortical lesion might affect the activities of PrV neurons. In the cortex-lesioned rats, (Sanchez-Jimenez et al. 2009) reported that sensory responses of the PrV neurons were decreased and that no oscillatory activity was observed in the PrV. These results support that the increased sensory responses and oscillatory firing of VPM and TRN neurons in the cortex-lesioned rats were mainly caused by the deprivation of direct corticothalamic inputs. Furthermore, since it is known that thalamic nuclei receive cortical inputs from neurons in both layer 5 and 6, one might suspect that the effects of the present cortical lesion on the VPM and TRN neurons are mediated by descending axons of layer 5 neurons. However, S1 layer 5 neurons do not innervate the VPM or TRN but massively project to the POm (Veinante et al. 2000). Given that layer 6 neurons constitute the vast majority of direct corticothalamic connections from S1, it is feasible that the effects of the cortical lesion on VPM and TRN neurons were mainly related to functions of layer 6 neurons. Moreover, we should also consider that VPM neurons in a barreloid might receive influence not only from the main barrel column homologous to the barreloid but also from surrounding barrel columns adjacent to the homologous barrel. It has been reported that adjacent barrel columns may modulate activities of barreloid neurons via TRN neurons or border-transgressing dendrites of barreloid neurons (Varga et al. 2002; Lavallée and Deschênes 2004; Li and Ebner 2007). Since our cortical lesion was not restricted to a single barrel column and covered almost the whole barrel cortex, the results of the cortical lesion should be regarded to contain effects of ablation of both the homologous barrel column and surrounding barrel columns. Future experiments in which activities of layer 6 corticothalamic neurons or neurons in a single barrel column

are specifically and acutely controlled (e.g. by optogenetics) may contribute to strictly identifying the role of these neurons.

Concluding remarks

Our cortical lesion experiments show that deprivation of corticothalamic afferents do affect the firing mode, and hence sensory gain and response probability and spontaneous firing patterns as well, of thalamocortical neurons during wakefulness. The results indicate that the corticothalamic modulators are indispensable for shaping normal sensory responses in the thalamus. The profound impact of corticothalamic input on thalamic activities presented here indicates that the thalamus is not a simple relay. Rather, the thalamus and cortex may constitute a highly integrated processing unit that dynamically regulates thalamocortical transmission of sensory information according to behavioral contexts.

Acknowledgements

We thank Profs R. Guillery and J.P. Bolam, Drs A.S. Mitchell, M. Murayama, N. Nakashima, Y. Hirai, and Y.R. Tanaka for helpful comments and discussion, Mr S. Momma for technical support, Profs K. Nakamura and Y. Isomura for technical advice. This work was supported by Grants-in-Aid for Scientific Research from Ministry of Education, Culture, Sports, Science, and Technology (23135519, 24500409, 15H04266 to T.F.; 15K19274 to D.H.; 26430015, 15H01663 to K.C.N.; 15K14333, 15H01430, 16H01426, 16H04663 to H.H.).

Conflict of Interest

The authors declare no competing financial interests.

References

- Alitto HJ, Usrey WM (2003) Corticothalamic feedback and sensory processing. *Curr Opin Neurobiol* 13:440–445.
- Andolina IM, Jones HE, Wang W, Sillito AM (2007) Corticothalamic feedback enhances stimulus response precision in the visual system. *Proc Natl Acad Sci USA* 104:1685–1690. doi: 10.1073/pnas.0609318104
- Bal T, von Krosigk M, McCormick DA (1995a) Role of the ferret perigeniculate nucleus in the generation of synchronized oscillations in vitro. *J Physiol (Lond)* 483:665–685.
- Bal T, von Krosigk M, McCormick DA (1995b) Synaptic and membrane mechanisms underlying synchronized oscillations in the ferret lateral geniculate nucleus in vitro. *J Physiol (Lond)* 483:641–663.
- Bourassa J, Pinault D, Deschênes M (1995) Corticothalamic projections from the cortical barrel field to the somatosensory thalamus in rats: a single-fibre study using biocytin as an anterograde tracer. *Eur J Neurosci* 7:19–30.
- Briggs F, Usrey WM (2008) Emerging views of corticothalamic function. *Curr Opin Neurobiol* 18:403–407. doi: 10.1016/j.conb.2008.09.002
- Briggs F, Usrey WM (2011) Corticogeniculate feedback and visual processing in the primate. *J Physiol* 589:33–40. doi: 10.1113/jphysiol.2010.193599
- Constantinople CM, Bruno RM (2013) Deep cortical layers are activated directly by thalamus. *Science* 340:1591–1594. doi: 10.1126/science.1236425
- Contreras D, Destexhe A, Sejnowski TJ, Steriade M (1996) Control of spatiotemporal coherence of a thalamic oscillation by corticothalamic feedback. *Science* 274:771–774.

Contreras D, Destexhe A, Sejnowski TJ, Steriade M (1997) Spatiotemporal patterns of spindle oscillations in cortex and thalamus. *J Neurosci* 17:1179–1196.

Crandall SR, Cruikshank SJ, Connors BW (2015) A corticothalamic switch: controlling the thalamus with dynamic synapses. *Neuron* 86:768–782. doi: 10.1016/j.neuron.2015.03.040

de Kock CPJ, Bruno RM, Spors H, Sakmann B (2007) Layer- and cell-type-specific suprathreshold stimulus representation in rat primary somatosensory cortex. *J Physiol* 581:139–154. doi: 10.1113/jphysiol.2006.124321

de Labra C, Rivadulla C, Grieve K, et al (2007) Changes in visual responses in the feline dLGN: selective thalamic suppression induced by transcranial magnetic stimulation of V1. *Cereb Cortex* 17:1376–1385. doi: 10.1093/cercor/bhl048

Denman DJ, Contreras D (2015) Complex effects on in vivo visual responses by specific projections from mouse cortical layer 6 to dorsal lateral geniculate nucleus. *J Neurosci* 35:9265–9280. doi: 10.1523/JNEUROSCI.0027-15.2015

Deschênes M, Veinante P, Zhang ZW (1998) The organization of corticothalamic projections: reciprocity versus parity. *Brain Res Brain Res Rev* 28:286–308.

Diamond ME, Armstrong-James M, Budway MJ, Ebner FF (1992) Somatic sensory responses in the rostral sector of the posterior group (POm) and in the ventral posterior medial nucleus (VPM) of the rat thalamus: dependence on the barrel field cortex. *J Comp Neurol* 319:66–84. doi: 10.1002/cne.903190108

Einevoll GT, Pettersen KH, Devor A, et al (2007) Laminar population analysis: estimating firing rates and evoked synaptic activity from multielectrode recordings in rat barrel cortex. *J Neurophysiol* 97:2174–2190. doi: 10.1152/jn.00845.2006

Fanselow EE, Sameshima K, Baccala LA, Nicolelis MA (2001) Thalamic bursting in rats during different awake behavioral states. *Proc Natl Acad Sci USA* 98:15330–15335. doi: 10.1073/pnas.261273898

Fujiyama F, Furuta T, Kaneko T (2001) Immunocytochemical localization of candidates for vesicular glutamate transporters in the rat cerebral cortex. *J Comp Neurol* 435:379–387.

Furuta T, Deschênes M, Kaneko T (2011) Anisotropic distribution of thalamocortical boutons in barrels. *J Neurosci* 31:6432–6439. doi: 10.1523/JNEUROSCI.6154-10.2011

Furuta T, Urbain N, Kaneko T, Deschênes M (2010) Corticofugal control of vibrissa-sensitive neurons in the interpolaris nucleus of the trigeminal complex. *J Neurosci* 30:1832–1838. doi: 10.1523/JNEUROSCI.4274-09.2010

Ghosh S, Murray GM, Turman AB, Rowe MJ (1994) Corticothalamic influences on transmission of tactile information in the ventroposterolateral thalamus of the cat: effect of reversible inactivation of somatosensory cortical areas I and II. *Exp Brain Res* 100:276–286.

Gil Z, Connors BW, Amitai Y (1997) Differential regulation of neocortical synapses by neuromodulators and activity. *Neuron* 19:679–686.

Guido W, Lu SM, Sherman SM (1992) Relative contributions of burst and tonic responses to the receptive field properties of lateral geniculate neurons in the cat. *J Neurophysiol* 68:2199–2211.

Guido W, Weyand T (1995) Burst responses in thalamic relay cells of the awake behaving cat. *J Neurophysiol* 74:1782–1786.

Holm S (1979) A simple sequentially rejective multiple test procedure. *Scand J Stat* 6:65–70.

- Jahnsen H, Llinás R (1984a) Electrophysiological properties of guinea-pig thalamic neurones: an in vitro study. *J Physiol* 349:205–226.
- Jahnsen H, Llinás R (1984b) Ionic basis for the electro-responsiveness and oscillatory properties of guinea-pig thalamic neurones in vitro. *J Physiol* 349:227–247.
- Jones HE, Andolina IM, Ahmed B, et al (2012) Differential feedback modulation of center and surround mechanisms in parvocellular cells in the visual thalamus. *J Neurosci* 32:15946–15951. doi: 10.1523/JNEUROSCI.0831-12.2012
- Kalil RE, Chase R (1970) Corticofugal influence on activity of lateral geniculate neurons in the cat. *J Neurophysiol* 33:459–474.
- Kaneko T, Caria MA, Asanuma H (1994) Information processing within the motor cortex. II. Intracortical connections between neurons receiving somatosensory cortical input and motor output neurons of the cortex. *J Comp Neurol* 345:172–184. doi: 10.1002/cne.903450203
- Kaneko T, Saeki K, Lee T, Mizuno N (1996) Improved retrograde axonal transport and subsequent visualization of tetramethylrhodamine (TMR) -dextran amine by means of an acidic injection vehicle and antibodies against TMR. *J Neurosci Methods* 65:157–165.
- Kim U, Sanchez-Vives MV, McCormick DA (1997) Functional dynamics of GABAergic inhibition in the thalamus. *Science* 278:130–134.
- King JL, Lowe MP, Stover KR, et al (2016) Adaptive processes in thalamus and cortex revealed by silencing of primary visual cortex during contrast adaptation. *Curr Biol* 26:1295–1300. doi: 10.1016/j.cub.2016.03.018

Kuramoto E, Furuta T, Nakamura KC, et al (2009) Two types of thalamocortical projections from the motor thalamic nuclei of the rat: a single neuron-tracing study using viral vectors. *Cereb Cortex* 19:2065–2077. doi: 10.1093/cercor/bhn231

Kwegyir-Afful EE, Simons DJ (2009) Subthreshold receptive field properties distinguish different classes of corticothalamic neurons in the somatosensory system. *J Neurosci* 29:964–972. doi: 10.1523/JNEUROSCI.3924-08.2009

Lacey CJ, Bolam JP, Magill PJ (2007) Novel and distinct operational principles of intralaminar thalamic neurons and their striatal projections. *J Neurosci* 27:4374–4384. doi: 10.1523/JNEUROSCI.5519-06.2007

Lavallée P, Deschênes M (2004) Dendroarchitecture and lateral inhibition in thalamic barreloids. *J Neurosci* 24:6098–6105. doi: 10.1523/JNEUROSCI.0973-04.2004

Lavallée P, Urbain N, Dufresne C, et al (2005) Feedforward inhibitory control of sensory information in higher-order thalamic nuclei. *J Neurosci* 25:7489–7498. doi: 10.1523/JNEUROSCI.2301-05.2005

Lee S, Carvell GE, Simons DJ (2008) Motor modulation of afferent somatosensory circuits. *Nat Neurosci* 11:1430–1438. doi: 10.1038/nn.2227

Lee SM, Friedberg MH, Ebner FF (1994) The role of GABA-mediated inhibition in the rat ventral posterior medial thalamus. I. Assessment of receptive field changes following thalamic reticular nucleus lesions. *J Neurophysiol* 71:1702–1715.

Li L, Ebner FF (2007) Cortical modulation of spatial and angular tuning maps in the rat thalamus. *J Neurosci* 27:167–179. doi: 10.1523/JNEUROSCI.4165-06.2007

Li Y, Ibrahim LA, Liu B, et al (2013) Linear transformation of thalamocortical input by intracortical excitation. *Nat Neurosci* 16:1324–1330. doi: 10.1038/nn.3494

Lien AD, Scanziani M (2013) Tuned thalamic excitation is amplified by visual cortical circuits. *Nat Neurosci* 16:1315–1323. doi: 10.1038/nn.3488

Liu XB, Honda CN, Jones EG (1995) Distribution of four types of synapse on physiologically identified relay neurons in the ventral posterior thalamic nucleus of the cat. *J Comp Neurol* 352:69–91. doi: 10.1002/cne.903520106

Llinás RR, Steriade M (2006) Bursting of thalamic neurons and states of vigilance. *J Neurophysiol* 95:3297–3308. doi: 10.1152/jn.00166.2006

Lo FS, Lu SM, Sherman SM (1991) Intracellular and extracellular in vivo recording of different response modes for relay cells of the cat's lateral geniculate nucleus. *Exp Brain Res* 83:317–328.

Lu SM, Guido W, Sherman SM (1992) Effects of membrane voltage on receptive field properties of lateral geniculate neurons in the cat: contributions of the low-threshold Ca²⁺ conductance. *J Neurophysiol* 68:2185–2198.

Malmierca E, Chaves-Coira I, Rodrigo-Angulo M, Nuñez A (2014) Corticofugal projections induce long-lasting effects on somatosensory responses in the trigeminal complex of the rat. *Front Syst Neurosci* 8:100. doi: 10.3389/fnsys.2014.00100

Marlinski V, Beloozerova IN (2014) Burst firing of neurons in the thalamic reticular nucleus during locomotion. *J Neurophysiol* 112:181–192. doi: 10.1152/jn.00366.2013

Massaux A, Dutrieux G, Cotillon-Williams N, et al (2004) Auditory thalamus bursts in anesthetized and non-anesthetized states: contribution to functional properties. *J Neurophysiol* 91:2117–2134. doi: 10.1152/jn.00970.2003

Massaux A, Edeline J-M (2003) Bursts in the medial geniculate body: a comparison between anesthetized and unanesthetized states in guinea pig. *Exp Brain Res* 153:573–578. doi: 10.1007/s00221-003-1516-3

Maunsell JH, Gibson JR (1992) Visual response latencies in striate cortex of the macaque monkey. *J Neurophysiol* 68:1332–1344.

McAlonan K, Cavanaugh J, Wurtz RH (2008) Guarding the gateway to cortex with attention in visual thalamus. *Nature* 456:391–394. doi: 10.1038/nature07382

McCormick DA, von Krosigk M (1992) Corticothalamic activation modulates thalamic firing through glutamate “metabotropic” receptors. *Proc Natl Acad Sci USA* 89:2774–2778.

Mease RA, Krieger P, Groh A (2014) Cortical control of adaptation and sensory relay mode in the thalamus. *Proc Natl Acad Sci USA* 111:6798–6803. doi: 10.1073/pnas.1318665111

Mitra PP, Pesaran B (1999) Analysis of dynamic brain imaging data. *Biophys J* 76:691–708. doi: 10.1016/S0006-3495(99)77236-X

Morison RS, Bassett DL (1945) Electrical activity of the thalamus and basal ganglia in decorticate cats. *J Neurophysiol* 8:309–314.

Murphy PC, Sillito AM (1987) Corticofugal feedback influences the generation of length tuning in the visual pathway. *Nature* 329:727–729. doi: 10.1038/329727a0

Nakamura KC, Sharott A, Magill PJ (2014) Temporal coupling with cortex distinguishes spontaneous neuronal activities in identified basal ganglia-recipient and cerebellar-recipient zones of the motor thalamus. *Cereb Cortex* 24:81–97. doi: 10.1093/cercor/bhs287

O’Connor DH, Fukui MM, Pinsk MA, Kastner S (2002) Attention modulates responses in the human lateral geniculate nucleus. *Nat Neurosci* 5:1203–1209. doi: 10.1038/nn957

Olsen SR, Bortone DS, Adesnik H, Scanziani M (2012) Gain control by layer six in cortical circuits of vision. *Nature* 483:47–52. doi: 10.1038/nature10835

- Pinault D (1996) A novel single-cell staining procedure performed in vivo under electrophysiological control: morpho-functional features of juxtacellularly labeled thalamic cells and other central neurons with biocytin or Neurobiotin. *J Neurosci Methods* 65:113–136.
- Plomp G, Quairiaux C, Kiss JZ, et al (2014) Dynamic connectivity among cortical layers in local and large-scale sensory processing. *Eur J Neurosci* 40:3215–3223. doi: 10.1111/ejn.12687
- Przybylski AW, Gaska JP, Foote W, Pollen DA (2000) Striate cortex increases contrast gain of macaque LGN neurons. *Vis Neurosci* 17:485–494.
- Ramcharan EJ, Gnadt JW, Sherman SM (2000) Burst and tonic firing in thalamic cells of unanesthetized, behaving monkeys. *Vis Neurosci* 17:55–62.
- Reichova I, Sherman SM (2004) Somatosensory corticothalamic projections: distinguishing drivers from modulators. *J Neurophysiol* 92:2185–2197. doi: 10.1152/jn.00322.2004
- Rivadulla C, Martínez LM, Varela C, Cudeiro J (2002) Completing the corticofugal loop: a visual role for the corticogeniculate type 1 metabotropic glutamate receptor. *J Neurosci* 22:2956–2962.
- Roy NC, Bessaih T, Contreras D (2011) Comprehensive mapping of whisker-evoked responses reveals broad, sharply tuned thalamocortical input to layer 4 of barrel cortex. *J Neurophysiol* 105:2421–2437. doi: 10.1152/jn.00939.2010
- Sakata S, Harris KD (2009) Laminar structure of spontaneous and sensory-evoked population activity in auditory cortex. *Neuron* 64:404–418. doi: 10.1016/j.neuron.2009.09.020

Sanchez-Jimenez A, Panetsos F, Murciano A (2009) Early frequency-dependent information processing and cortical control in the whisker pathway of the rat: electrophysiological study of brainstem nuclei principalis and interpolaris. *Neuroscience* 160:212–226. doi: 10.1016/j.neuroscience.2009.01.075

Sherman SM (2001a) Tonic and burst firing: dual modes of thalamocortical relay. *Trends Neurosci* 24:122–126.

Sherman SM (2001b) A wake-up call from the thalamus. *Nat Neurosci* 4:344–346. doi: 10.1038/85973

Sherman SM, Guillery RW (1996) Functional organization of thalamocortical relays. *J Neurophysiol* 76:1367–1395.

Sherman SM, Guillery RW (1998) On the actions that one nerve cell can have on another: distinguishing “drivers” from “modulators.” *Proc Natl Acad Sci USA* 95:7121–7126.

Sherman SM, Guillery RW (2006) *Exploring the thalamus and its role in cortical function*, 2nd edn. MIT Press, Cambridge (MA)

Sherman SM, Guillery RW (2013) *Functional connections of cortical areas: A new view from the thalamus*. MIT Press, Cambridge

Sheroziya M, Timofeev I (2014) Global intracellular slow-wave dynamics of the thalamocortical system. *J Neurosci* 34:8875–8893. doi: 10.1523/JNEUROSCI.4460-13.2014

Simons DJ (1978) Response properties of vibrissa units in rat SI somatosensory neocortex. *J Neurophysiol* 41:798–820.

Slézia A, Hangya B, Ulbert I, Acsády L (2011) Phase advancement and nucleus-specific timing of thalamocortical activity during slow cortical oscillation. *J Neurosci* 31:607–617. doi: 10.1523/JNEUROSCI.3375-10.2011

Steriade M (2001) To burst, or rather, not to burst. *Nat Neurosci* 4:671. doi: 10.1038/89434

Steriade M, Deschênes M, Domich L, Mulle C (1985) Abolition of spindle oscillations in thalamic neurons disconnected from nucleus reticularis thalami. *J Neurophysiol* 54:1473–1497.

Steriade M, Domich L, Oakson G, Deschênes M (1987) The deafferented reticular thalamic nucleus generates spindle rhythmicity. *J Neurophysiol* 57:260–273.

Swadlow HA, Gusev AG (2001) The impact of “bursting” thalamic impulses at a neocortical synapse. *Nat Neurosci* 4:402–408. doi: 10.1038/86054

Tanaka YR, Tanaka YH, Konno M, et al (2011) Local connections of excitatory neurons to corticothalamic neurons in the rat barrel cortex. *J Neurosci* 31:18223–18236. doi: 10.1523/JNEUROSCI.3139-11.2011

Temereanca S, Simons DJ (2004) Functional topography of corticothalamic feedback enhances thalamic spatial response tuning in the somatosensory whisker/barrel system. *Neuron* 41:639–651.

Thomson AM (2010) Neocortical layer 6, a review. *Front Neuroanat* 4:13. doi: 10.3389/fnana.2010.00013

Timofeev I, Bazhenov M, Seigneur J, Sejnowski T (2012) Neuronal synchronization and thalamocortical rhythms in sleep, wake and epilepsy. In: Noebels JL, Avoli M, Rogawski MA, et al. (eds) *Jasper’s basic mechanisms of the epilepsies*, 4th edn. National Center for Biotechnology Information, Bethesda (MD)

- Urbain N, Deschênes M (2007) A new thalamic pathway of vibrissal information modulated by the motor cortex. *J Neurosci* 27:12407–12412. doi: 10.1523/JNEUROSCI.2914-07.2007
- Urbain N, Salin PA, Libourel P-A, et al (2015) Whisking-Related Changes in Neuronal Firing and Membrane Potential Dynamics in the Somatosensory Thalamus of Awake Mice. *Cell Rep* 13:647–656. doi: 10.1016/j.celrep.2015.09.029
- Ushimaru M, Ueta Y, Kawaguchi Y (2012) Differentiated participation of thalamocortical subnetworks in slow/spindle waves and desynchronization. *J Neurosci* 32:1730–1746. doi: 10.1523/JNEUROSCI.4883-11.2012
- Varga C, Sík A, Lavallée P, Deschênes M (2002) Dendroarchitecture of relay cells in thalamic barreloids: a substrate for cross-whisker modulation. *J Neurosci* 22:6186–6194.
- Veinante P, Lavallée P, Deschênes M (2000) Corticothalamic projections from layer 5 of the vibrissal barrel cortex in the rat. *J Comp Neurol* 424:197–204.
- Vélez-Fort M, Rousseau CV, Niedworok CJ, et al (2014) The stimulus selectivity and connectivity of layer six principal cells reveals cortical microcircuits underlying visual processing. *Neuron* 83:1431–1443. doi: 10.1016/j.neuron.2014.08.001
- Villablanca J, Schlag J (1968) Cortical control of thalamic spindle waves. *Exp Neurol* 20:432–442.
- von Krosigk M, Bal T, McCormick DA (1993) Cellular mechanisms of a synchronized oscillation in the thalamus. *Science* 261:361–364.
- Wang W, Jones HE, Andolina IM, et al (2006) Functional alignment of feedback effects from visual cortex to thalamus. *Nat Neurosci* 9:1330–1336. doi: 10.1038/nn1768

Welker E, Armstrong-James M, Van der Loos H, Kraftsik R (1993) The mode of activation of a barrel column: response properties of single units in the somatosensory cortex of the mouse upon whisker deflection. *Eur J Neurosci* 5:691–712.

Weyand TG, Boudreaux M, Guido W (2001) Burst and tonic response modes in thalamic neurons during sleep and wakefulness. *J Neurophysiol* 85:1107–1118.

Yan J, Suga N (1996) Corticofugal modulation of time-domain processing of biosonar information in bats. *Science* 273:1100–1103.

Zhan XJ, Cox CL, Rinzel J, Sherman SM (1999) Current clamp and modeling studies of low-threshold calcium spikes in cells of the cat's lateral geniculate nucleus. *J Neurophysiol* 81:2360–2373.

Zhang Y, Suga N, Yan J (1997) Corticofugal modulation of frequency processing in bat auditory system. *Nature* 387:900–903. doi: 10.1038/43180

Figures

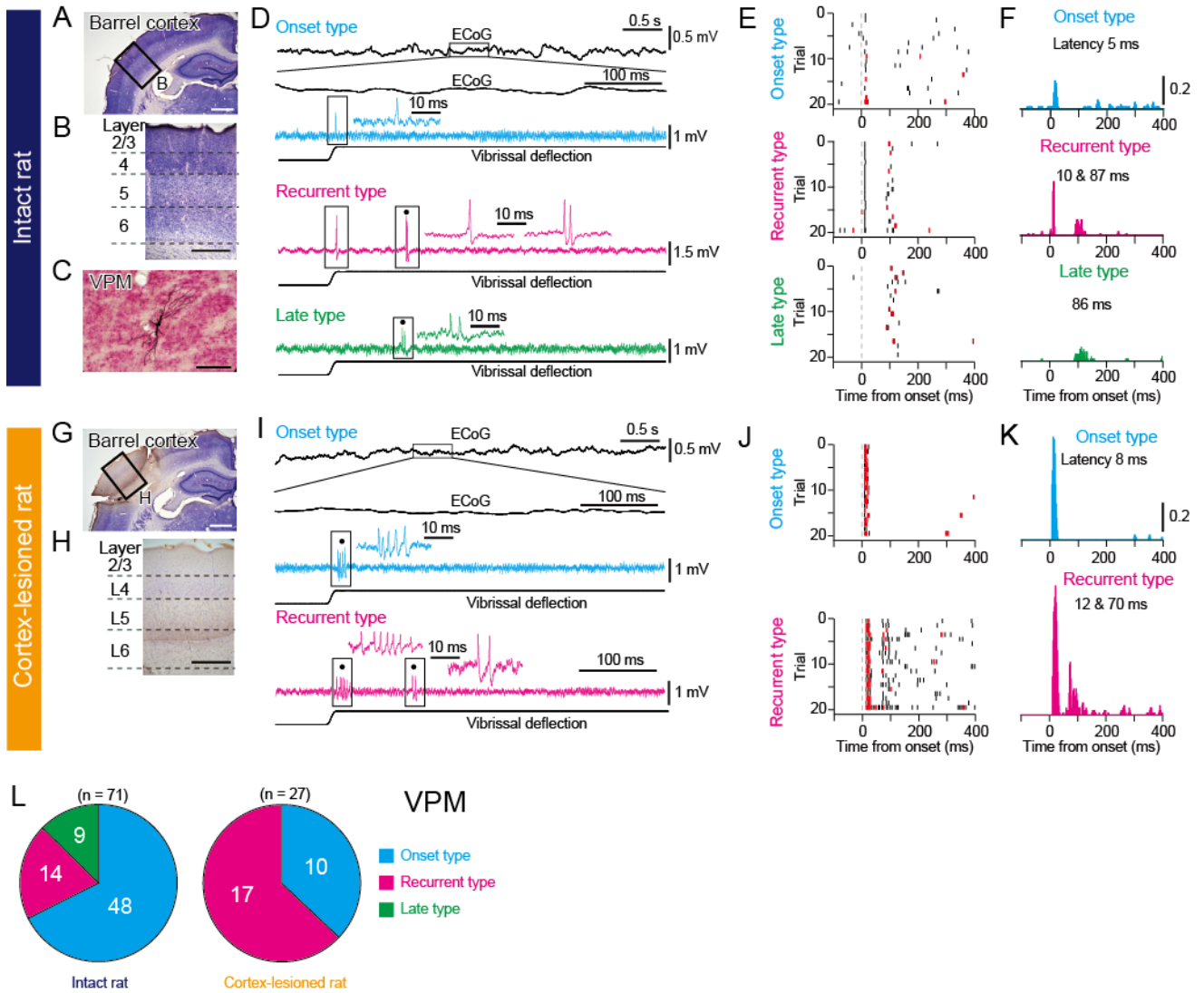


Figure 1
Typical response profiles of VPM neurons to vibrissal deflection in intact and cortex-lesioned rats .

Figure 1. Typical response profiles of VPM neurons to vibrissal deflection in intact and cortex-lesioned rats. *A.* A micrograph of a Nissl-stained coronal section including the intact barrel cortex. Scale bar: 1 mm. *B.* The barrel cortex (the rectangle in *A*) is shown at a higher magnification with layers identified according to Nissl staining. Scale bar: 200 μm . *C.* A representative micrograph illustrates the somatodendritic structure of a VPM neuron. Scale bar: 100 μm . *D.* Cyan, magenta, and green traces, respectively, show typical response patterns of onset, recurrent, and late types of VPM neurons to principal vibrissal deflection in intact rats. Simultaneously recorded ECoG is also shown for the onset type neurons at two time scales (top). Stimulus duration: 500 ms. Filled circles indicate LTS bursts. *E.* Raster plots represent the spike discharges of the same neurons shown in *D* with black and red markers for non-burst spikes and spikes included in LTS bursts, respectively. The dashed gray vertical line represents the time of the stimulus onset. *F.* PSTHs (bin width, 2 ms) represent responses of the same neurons as in *D and E* to 20 stimulations. *G.* Focal lesion of the barrel cortex by topical application of silver nitrate on the pia. The extent of the lesion is evident as a reduction of Nissl staining. Scale bar: 1 mm. *H.* Paucity of Nissl staining illustrates that the lesion extended over the entire thickness of the barrel cortex (the rectangle in *G*). Scale bar: 200 μm . *I–K.* Similar to *D–F*, but for cortex-lesioned rats. No late type VPM neuron was found in cortex-lesioned rats. *L.* Proportions of neuron types in the VPM ($n = 71$ cells for intact, $n = 27$ for cortex-lesioned rats, $*p < 0.05$, Fisher's exact test).

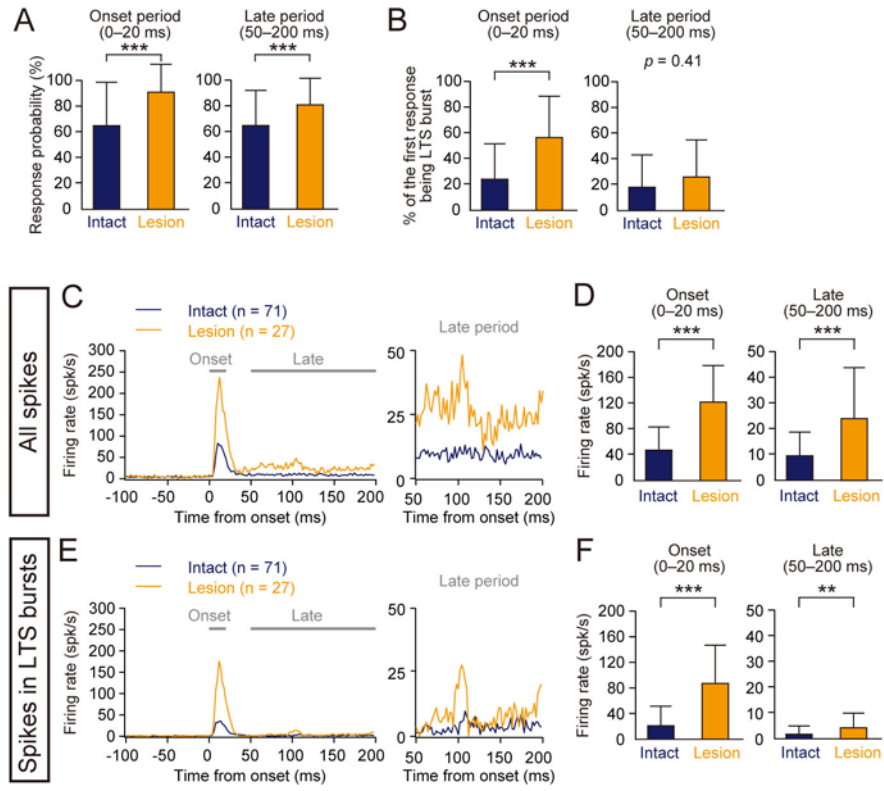


Figure 2

Comparison of sensory responses of VPM neurons between intact and cortex-lesioned rats.

Figure 2. Sensory responses of VPM neurons in intact and cortex-lesioned rats. A.

The response probabilities of VPM neurons to sensory stimulation are compared between the intact and cortex-lesioned rats for the onset (left) and late (right) periods. **B.** The percentages of the first response being a LTS burst during the onset (left) and late (right) periods are compared between the intact and cortex-lesioned rats. $***p < 0.001$, Mann-Whitney *U*-test in *A* and *B*. **C.** Population PSTHs show the averaged responses of all the VPM neurons to vibrissal deflection in intact and cortex-lesioned rats (left). A detailed view of the PSTHs during the late period are also shown (right; 50–200 ms after stimulus onset). **D.** The firing rates were higher in lesioned rats than in intact rats both in the onset period ($***p < 0.001$, Mann-Whitney *U*-test) and the late period ($***p < 0.001$, Mann-Whitney *U*-test). **E and F.** Similar to *C–D*, but only for spikes included in LTS bursts. Firing rates were higher in lesioned rats than in intact rats both in the onset period ($***p < 0.001$, Mann-Whitney *U*-test) and the late period ($**p < 0.01$, Mann-Whitney *U*-test) (*F*).

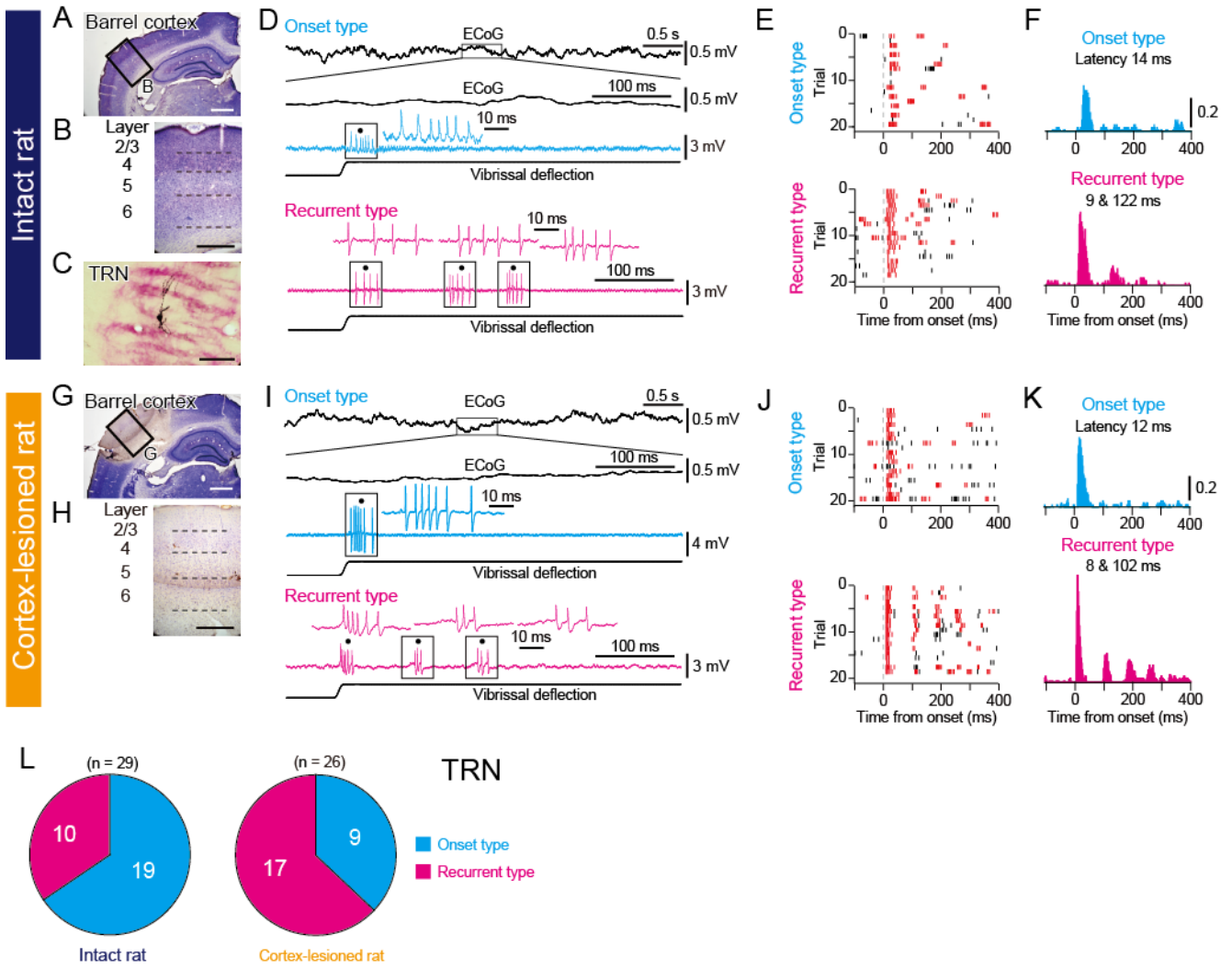


Figure 3
Typical response profiles of TRN neurons in intact and barrel-lesioned rats.

Figure 3. Typical response profiles of TRN neurons in intact and cortex-lesioned rats. **A.** A micrograph represents a Nissl-stained coronal section showing the intact barrel cortex. Scale bar: 1 mm. **B.** Layers of the barrel cortex are indicated. Scale bar: 200 μm . **C.** A representative micrograph illustrating the somatodendritic structure of a TRN neuron. Scale bar: 100 μm . **D.** Cyan and magenta traces, respectively, show characteristic response patterns of onset and recurrent types of TRN neurons to principal vibrissal deflection in intact rats. A simultaneously recorded ECoG is also shown for the onset type neurons (top). No late type neurons were found in the TRN. Stimulus duration: 500 ms. Filled circles indicate LTS bursts. **E.** Raster plots represent the spike discharges of the same neurons shown in *D* with black and red markers for non-burst spikes and spikes included in LTS bursts, respectively. The dashed gray vertical line represents the time at the stimulus onset. **F.** Each PSTH (bin width, 2 ms) represents responses of the same neuron as in *D* and *E* to 20 stimulations. **G.** Focal lesion of the barrel cortex by topical application of silver nitrate on the pia. The extent of the lesion is evident as a reduction of Nissl staining. Scale bar: 1 mm. **H.** Paucity of Nissl staining illustrates that the lesion extended over the entire thickness of the barrel cortex. Scale bar: 200 μm . **I–K.** Similar to *D–F*, but for the TRN of cortex-lesioned rats. **L.** Proportions of neuron types in the TRN ($n = 29$ cells for intact rats; $n = 26$ for cortex-lesioned rats; $*p < 0.05$, Fisher's exact test).

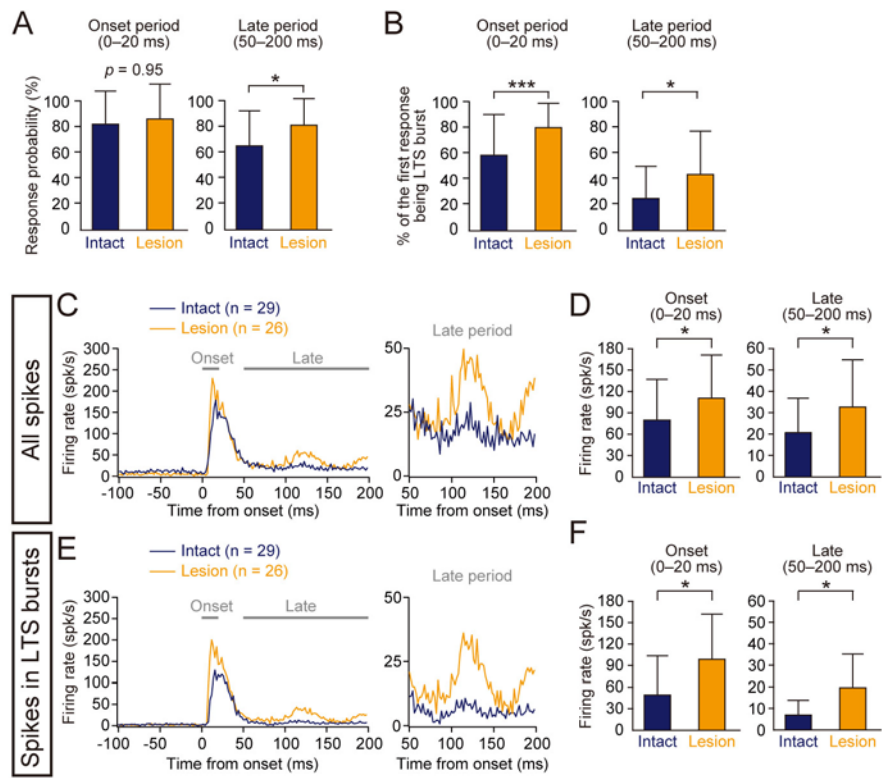


Figure 4
Sensory responses of TRN neurons in intact and cortex-lesioned rats.

Figure 4. Sensory responses of TRN neurons in intact and cortex-lesioned rats. A.

The response probabilities of TRN neurons to sensory stimulation are compared between the intact and cortex-lesioned rats for the onset period (left, $*p < 0.05$, Mann-Whitney *U*-test) and late the periods (right, $p = 0.95$, Mann-Whitney *U*-test). **B.** The percentages of the first response being an LTS burst during the onset (left) and late (right) periods are compared between the intact and cortex-lesioned rats. **C.** Population PSTHs show the average responses of all the TRN neurons to vibrissal deflection in intact and cortex-lesioned rats (left). PSTHs show a detailed view of the response during the late period (right; 50–200 ms after stimulus onset). **D.** The firing rates were higher in lesioned rats than in intact rats both in the onset period ($*p < 0.05$, Mann-Whitney *U*-test) and late period ($*p < 0.05$, Mann-Whitney *U*-test). **E and F.** Similar to C–D, but only for spikes included in LTS bursts. Firing rates were higher in lesioned rats than in intact rats in both the onset period ($*p < 0.05$, Mann-Whitney *U*-test) and late period ($*p < 0.05$, Mann-Whitney *U*-test) (*F*).

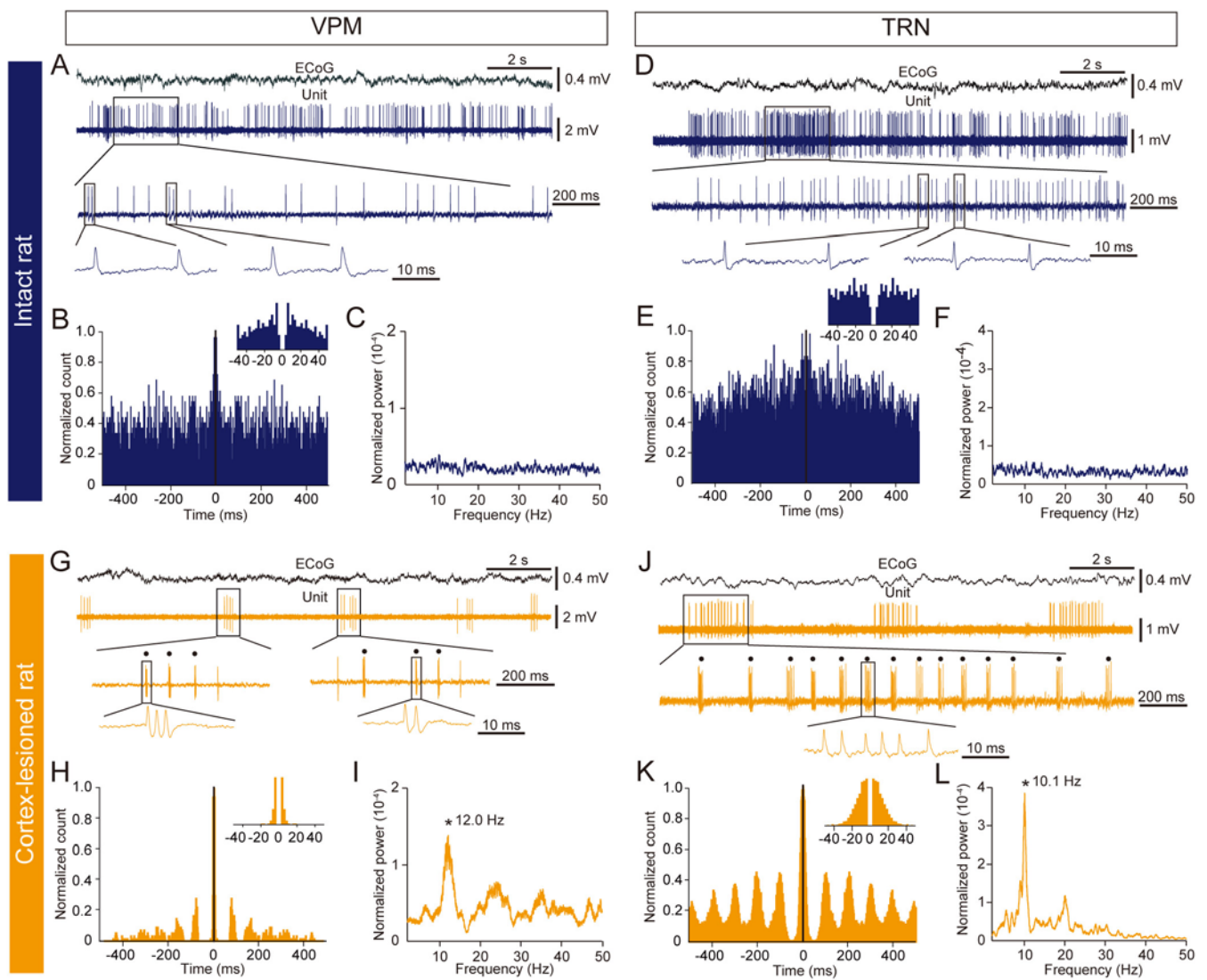


Figure 5
 Typical spontaneous firing patterns of VPM and TRN neurons in intact and cortex-lesioned rats.

Figure 5. Typical spontaneous firing patterns of VPM and TRN neurons in intact and cortex-lesioned rats. *A.* Spontaneous activity of a typical VPM neuron in an intact rat during quiet wakefulness is shown at three time scales with a simultaneously recorded ECoG at the top. Note that ECoG exhibits desynchronized cortical state. *B.* Autocorrelogram for 60 s of spike train of the same neuron as in *A* normalized to the maximum bin with a 2 ms resolution. Inset shows close-up of the autocorrelogram, illustrating a refractory period. *C.* Power spectrum of the spike train of the neuron in *A* and *B*. *D–F.* Similar to *A–C*, but for a typical TRN neuron of an intact rat. *G–L.* Similar to *A–C*, but for a typical VPM neuron (*G–I*) and TRN neuron (*J–L*) of cortex-lesioned rats. Filled circles in *G* and *J* indicate LTS bursts. Asterisks in *H* and *K* denote peaks in power spectra.

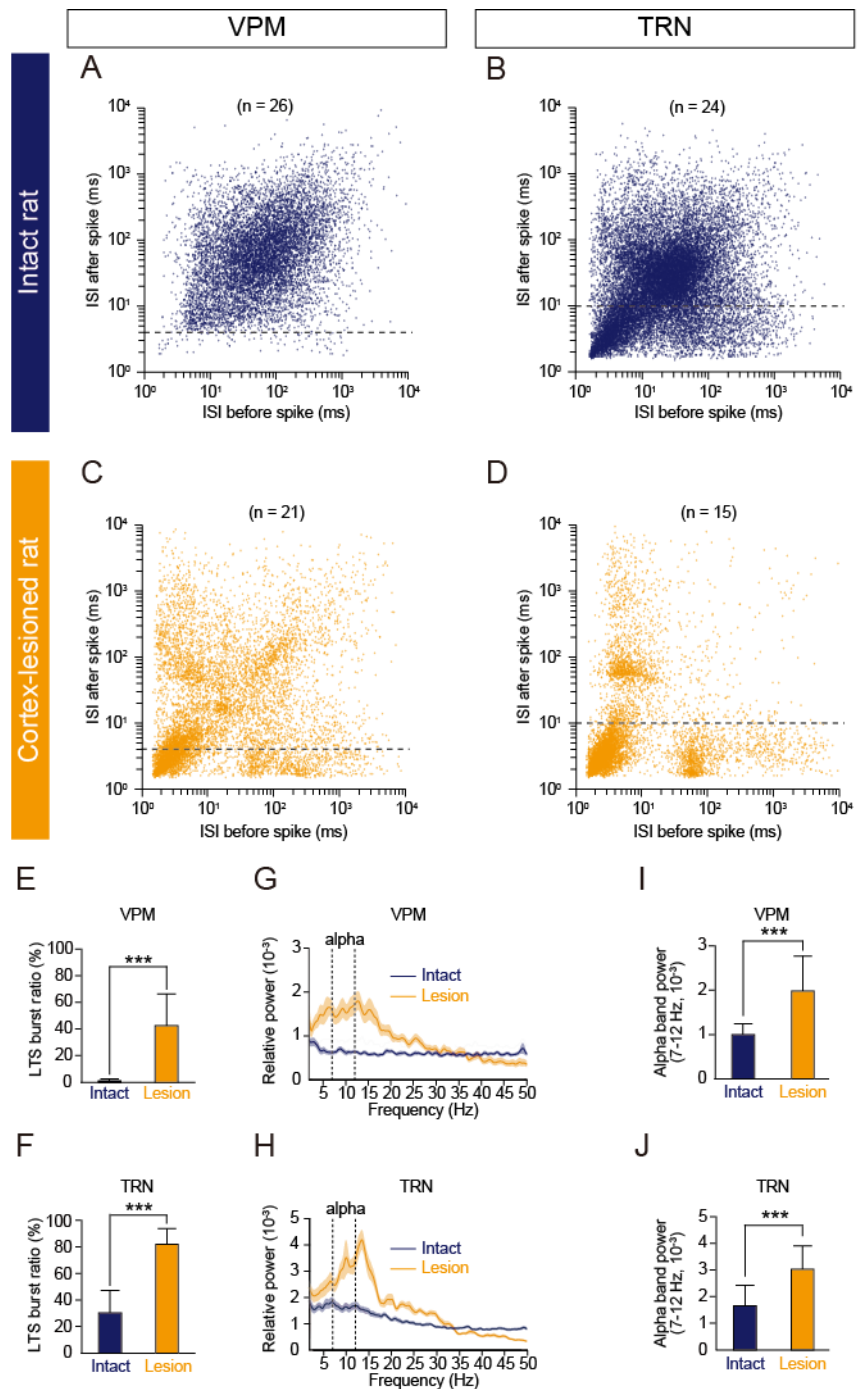


Figure 6
Spontaneous activities of VPM and TRN neurons in intact and cortex-lesioned rats.

Figure 6. Spontaneous activities of VPM and TRN neurons in intact and cortex-lesioned rats. *A–D.* Relationships between ISI before spike (*x* axis) and ISI after spike (*y* axis) for all of the recorded VPM and TRN neurons in intact and cortex-lesioned rats are presented (*A.* VPM of intact rat, $n = 26$ cells, *B.* TRN of intact rat, $n = 21$ cells, *C.* VPM of lesioned rat, $n = 24$ cells, *D.* TRN of lesioned rat, $n = 15$ cells). Each spike is represented by a single dot. Note the logarithmic axes. Dashed lines indicate thresholds used for detecting LTS bursts in the VPM and TRN; the first ISI in a burst must be <4 ms and <10 ms, respectively (see Materials and Methods for further details). *E and F.* The mean percentages of all spikes included in LTS bursts for all VPM neurons (intact rat, $n = 26$ cells; lesioned rat, $n = 21$ cells; $***p < 0.001$ in *E*) and all TRN neurons (intact rat, $n = 24$ cells; lesioned rat, $n = 15$ cells; $***p < 0.001$ in *F*) are compared between intact and lesioned rats. *G.* The mean power spectra of spike trains of all the VPM cells normalized by all frequency bins (bin size, 0.1 Hz; ranging 0.3–100 Hz). Shaded areas indicate ± 1 SEM. *I.* The mean alpha (7–12 Hz) power of all the VPM neurons is compared between intact and cortex-lesioned rats (intact rat, $n = 26$ cells; lesioned rat, $n = 21$ cells; $***p < 0.001$, Mann-Whitney U-test with Bonferroni–Holm correction). *H and J.* Similar to *G* and *I*, but for TRN neurons (intact rat, $n = 24$ cells; lesioned rat, $n = 15$ cells; $***p < 0.001$ in *I*, Mann-Whitney U-test with Bonferroni–Holm correction).

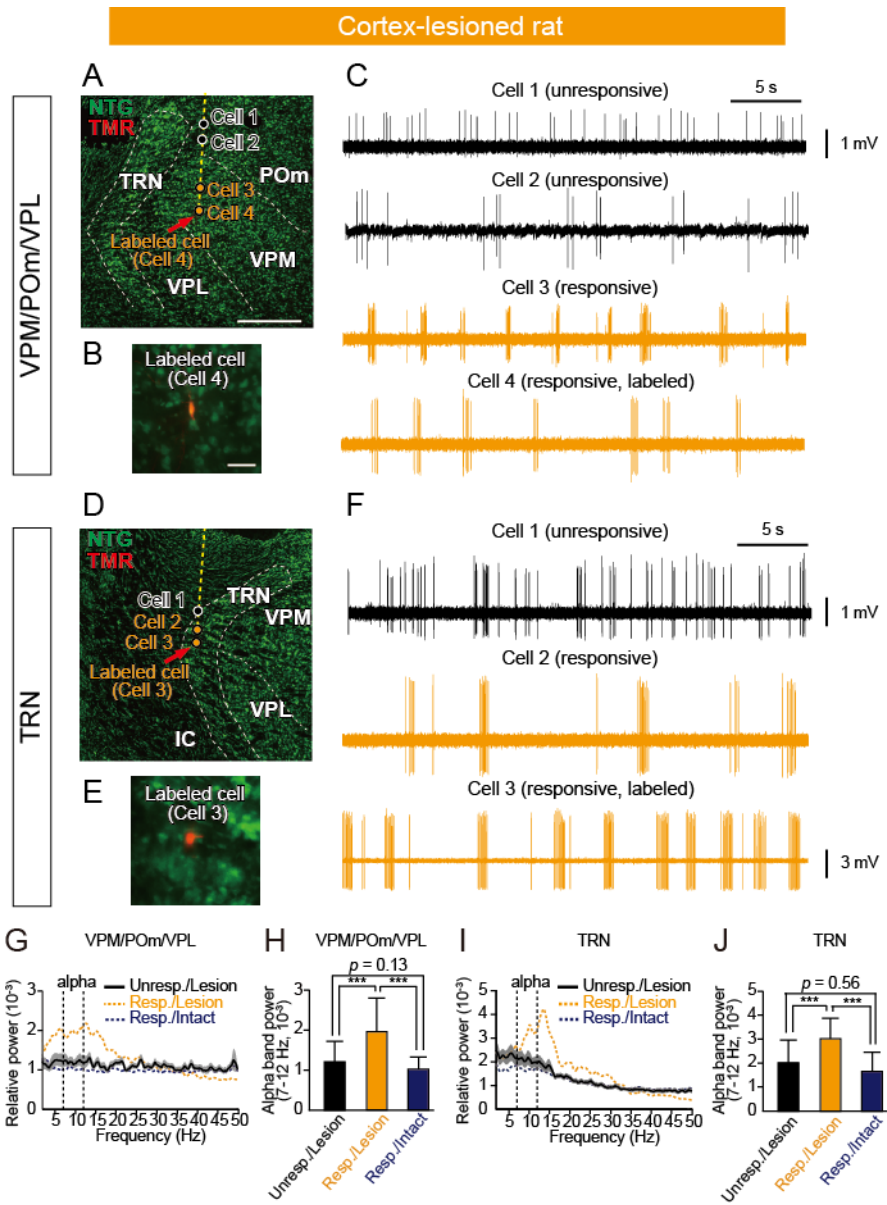


Figure 7

Spontaneous activities of vibrissa-responsive and unresponsive neurons in cortex-lesioned rats.

Figure 7. Spontaneous activities of vibrissa-responsive and -unresponsive neurons

in cortex-lesioned rats. **A.** Extrapolation of all the recording sites along an example penetration (yellow dashed line) through the POm and VPM is shown. At the end of the penetration, the last cell (Cell 4) responsive to vibrissal deflection was juxtacellularly labeled with a fluorescent tracer TMR (indicated by red arrows). In *post hoc* analyses, the positions of recorded neurons were extrapolated from the location of the labeled neurons and the depth measurements from the pia during recording, and were reconstructed on an image of the thalamus. Scale bar equals to 1.0 mm. **B.** A magnified micrograph of the TMR-labeled neuron in **A**. Scale bar equals to 100 μ m. **C.** Spontaneous activities of the recorded neurons in the penetration into the POm and VPM (represented in **A**) are shown. **D–F.** Similar to **A–C**, but for recordings from the TRN of a cortex-lesioned rat. **G.** The mean power spectra of spike trains of all neurons are compared between the vibrissa-unresponsive cells in the VPM/ POm/VPL (Unresp./Lesion, $n = 15$ cells) of cortex-lesioned rats, the vibrissa-responsive cells in the VPM of cortex-lesioned (Resp./Lesion, $n = 21$ cells) and the vibrissa-responsive VPM cells in intact rats (Resp./Intact, $n = 26$ cells). Shaded areas indicate ± 1 SEM. **H.** The mean alpha (7–12 Hz) power of the recorded neurons is compared between three groups (Unresp./Lesion, $n = 15$, Resp./Intact, $n = 26$, Resp./Lesion, $n = 21$, *** $p < 0.001$, Mann-Whitney U-test with Bonferroni–Holm correction). **I and J.** Similar to **G** and **H**, but for TRN neurons (Unresp./Lesion, $n = 14$ cells, Resp./Lesion, $n = 15$ cells, Resp./Intact, $n = 24$ cells, *** $p < 0.001$, Mann-Whitney U-test with Bonferroni–Holm correction).

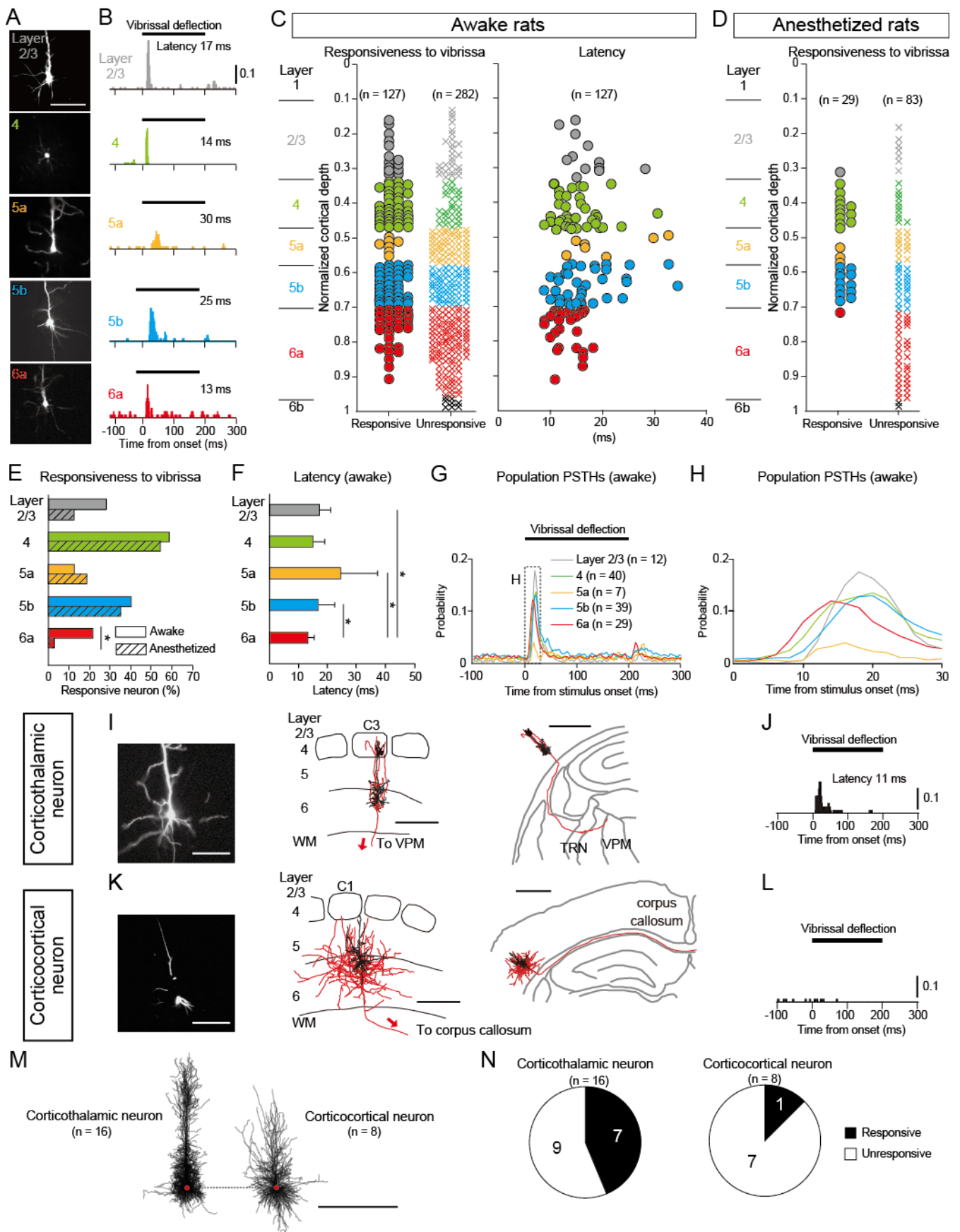


Figure 8
Corticothalamic neurons in layer 6a of the barrel cortex respond to vibrissal deflection with short latency during wakefulness.

Figure 8. Corticothalamic neurons in layer 6a of the barrel cortex respond to vibrissal deflection with a short latency during wakefulness. *A.* Micrographs of a typical TMR-labeled neuron in each layer of the barrel cortex. Scale bar: 100 μm . *B.* PSTHs illustrate the responses of the same neurons shown in *A* to deflection of the principal vibrissa in the preferred direction. *C.* The distributions of vibrissa-responsive and -unresponsive neurons are shown in relation to the normalized cortical depth (left). The response latencies of neurons with phasic responses are plotted against the normalized cortical depth (right). *D.* Depth distribution of neurons that showed a response or no response to vibrissal deflections under ketamine-xylazine anesthesia. *E.* The percentages of vibrissa-responsive neurons among all the recorded neurons in each layer in awake and anesthetized rats. The percentage of vibrissa-responsive neurons in layer 6a of anesthetized rats was significantly lower than that of awake rats ($*p < 0.05$, Fisher's exact test with Bonferroni–Holm correction). *F.* The average response latencies of neurons in each layer ($n = 12$ cells for layer 2/3, $n = 40$ for layer 4, $n = 7$ for layer 5a, $n = 39$ for layer 5b, $n = 29$ for layer 6a) are shown. The latency of layer 6a neurons was shorter than that of neurons in layers 2/3, 5a, and 5b ($*p < 0.05$, Mann-Whitney *U*-test with Bonferroni–Holm correction). *G.* Population PSTHs of neurons in each layer of the barrel cortex with a 2 ms bin. *H.* Same data as in *G* but showing the first 30 ms of the response. *I.* An example of identified corticothalamic projection neurons that sent efferent axons into the thalamic VPM. Scale bar: 200 μm (left), 500 μm (middle) and 1 mm (right). *J.* The same neuron in *I* showed an onset response to vibrissal deflection. *K.* An example of identified corticocortical projection neurons whose efferent axons project to the contralateral hemisphere through the corpus callosum. Scale bar: 200 μm (left), 500 μm (middle) and 1 mm (right). *L.* The same neuron as *K* did not respond to

vibrissal deflection. *M*. The soma and dendrites of 16 corticothalamic and 8 corticocortical neurons are overlaid, centered on their somata. *N*. The proportion of all identified corticothalamic and corticocortical neurons that are responsive.

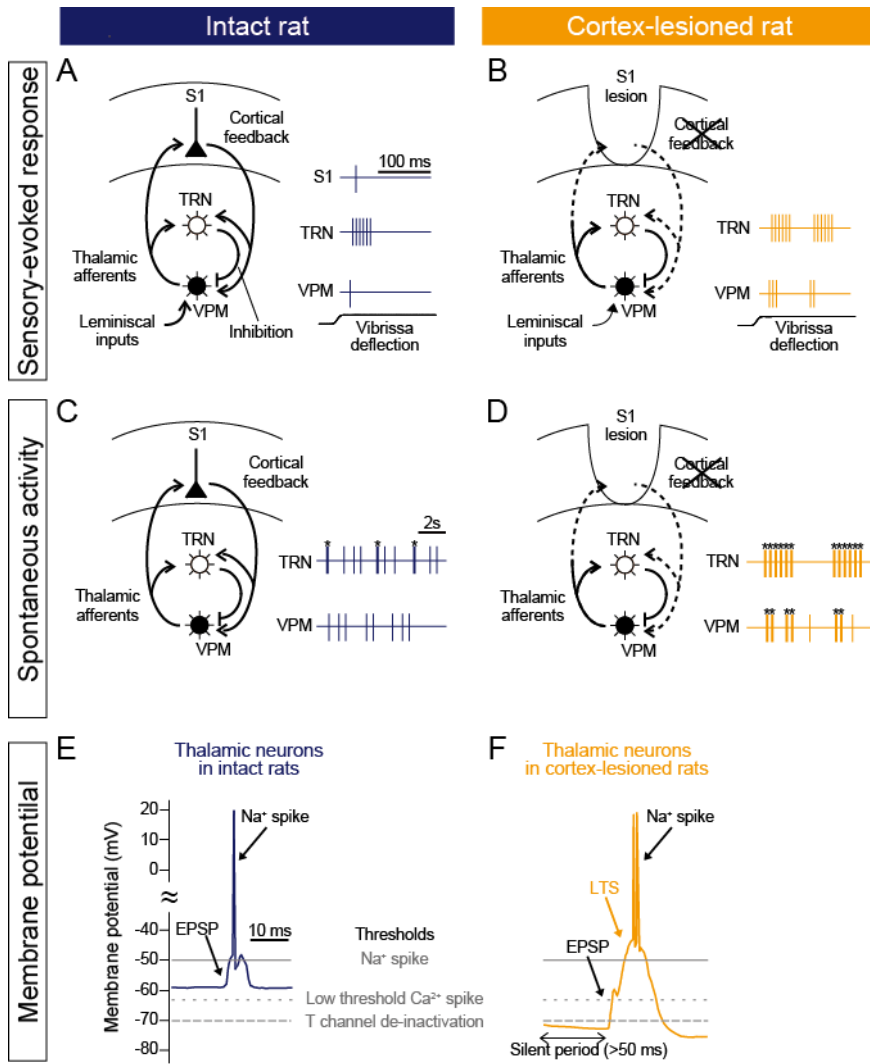


Figure 9
Schematic view of output dynamics of thalamic neurons
in intact and cortex-lesioned rats.

Figure 9. Schematic view of output dynamics of thalamic neurons in intact and cortex-lesioned rats. A-D. Summary of sensory-evoked and spontaneous activity of thalamic neurons in intact and cortex-lesioned rats. **A.** By way of VPM neurons, lemniscal inputs activate TRN and corticothalamic neurons in Layer 6 of the barrel cortex. In turn, corticothalamic neurons give feedback to the VPM and TRN neurons with a short latency. **B.** In cortex-lesioned rats, VPM and TRN neurons enhanced late responses to lemniscal inputs with LTS bursts. **C and D.** Spontaneous activity in VPM and TRN neurons in intact and cortex-lesioned rats. Filled circles indicate LTS bursts. **E.** Figure represents presumed membrane potential dynamics of thalamic neurons in intact rats. Horizontal lines indicate each threshold. **F.** Presumed dynamics of thalamic membrane potentials in cortex-lesioned rats.